8-2014

Temperature and Alloying Effects on the Mechanical Properties of Equiatomic FCC Solid Solution Alloys

Zhenggang Wu
University of Tennessee - Knoxville, zwu9@vols.utk.edu

To the Graduate Council:

I am submitting herewith a dissertation written by Zhenggang Wu entitled "Temperature and Alloying Effects on the Mechanical Properties of Equiatomic FCC Solid Solution Alloys." I have examined the final electronic copy of this dissertation for form and content and recommend that it be accepted in partial fulfillment of the requirements for the degree of Doctor of Philosophy, with a major in Materials Science and Engineering.

George M. Pharr, Major Professor

We have read this dissertation and recommend its acceptance:

Easo P. George, Madhu S. Madhukar, Hongbin Bei

Accepted for the Council:

Carolyn R. Hodges

Vice Provost and Dean of the Graduate School

(Original signatures are on file with official student records.)

Temperature and Alloying Effects on the Mechanical Properties of Equiatomic FCC Solid Solution Alloys

A Dissertation Presented for the

Doctor of Philosophy

Degree

The University of Tennessee, Knoxville

Zhenggang Wu

August 2014

DEDICATION

To my parents, Wu, Shantao and Li, Xianrong, my wife, Li, Hua, my son, Wu, Lize, my coming daughter, Wu, Liyan, my sister, Wu, Zhiling, my brothers, Wu, Longqiu and Wu, Yueteng, for their love and supports

ACKNOWLEDGEMENTS

I would like to express my sincere appreciation to Dr. George Pharr and Dr. Easo George for their scientific guidance, encouragement and kindness through out my study and completion of this dissertation. I am grateful to Dr. Hongbin Bei for his valuable suggestions and enormous support during the proceeding of the experiments. I would also like to thank Dr. Madhu Madhukar for serving on my committee.

I am also grateful to my fellow graduate students and staff members in the Department of Materials Science and Engineering, The University of Tennessee, Knoxville, and the Alloying Behavior and Design group, Oak Ridge National Laboratory for the wonderful time we spent together. All the members of Dr. Pharr's research group, past and present, deserve thanks for their help and friendship. Special gratitude goes to Dr. Caijun Su and Dr. Zhigang Wang whose kind help and support brought me much easier life during my staying in Knoxville. Great appreciation will also be shown to Dr. Xiaocun Sun from Office of Information Technology at the University of Tennessee for her helpful discussion on the statistical methods.

This research was sponsored by the Division of Materials Sciences and Engineering, Office of Basic Energy Sciences, U. S. Department of Energy.

ABSTRACT

Compared to decades-old theories of strengthening in dilute solid solutions, the mechanical behavior of concentrated solid solutions is relatively poorly understood. A special subset of these materials includes alloys in which the constituent elements are present in equal atomic proportions, including the high-entropy alloys of recent interest. A unique characteristic of equiatomic alloys is the absence of “solvent” and “solute” atoms, resulting in a breakdown of the textbook picture of dislocations moving through a solvent lattice and encountering discrete solute obstacles. To clarify the mechanical behavior of this interesting new class of materials, we investigate here a family of equiatomic binary, ternary, and quaternary alloys based on the elements Fe, Ni, Co, Cr, and Mn. These subsets were dropp-cast, homogenized, cold-rolled, and further annealed. The recovery, recrystallization, grain growth and phase stability of these alloys were investigated first to identify the alloys with pure FCC crystal structure and their stability and to determine the suitable thermomechanical processing needed to obtain desired microstructures. After this, the mechanical properties of the alloys with FCC crystal structure and comparable grain size were investigated as a function of temperature. The flow stresses were observed to depend to varying degrees on temperature. Lattice friction stress appears to contribute significantly to the temperature-dependent yield stress, possibly because the Peierls barrier height decreases with increasing temperature due to thermal vibration induced increase of dislocation width. In the early stages of plastic flow (5~13% strain, depending on material), the temperature dependence of strain hardening is due mainly to the shear modulus changing with temperature since the curves at different temperatures collapse when the shear modulus corrected flow stress is plotted against strain. In all equiatomic alloys, both strain hardening capability and ductility increase with decreasing temperature, and the formation of deformation twinning could

be an important comtribution to this. A statistical analysis is conducted to investigate the alloying (compositional) effects on the mechanical properties. The analysis suggests that, among the factors that have been investigated, the mechanical behavior is most highly correlated with the annealing twin density, which can have effects on strength and strain hardening behavior.

Table of Contents

LISTS OF TABLES

LISTS OF FIGURES

INTRODUCTION

This dissertation is based on three journal articles: 1) "Recovery, Recrystallization, Grain Growth and Phase Stability of a Family of FCC-Structured Multi-Component Equiatomic Solid Solution Alloys"; (2) "Temperature Dependence of the Mechanical Properties of Equiatomic Solid Solution Alloys with FCC Crystal Structures"; and (3) "Alloying Effects on the Mechanical Properties of Equiatomic FCC Solid Solution Alloys". The focus of these articles is to investigate the influence of temperature on the mechanical properties of single-phase equiatomic multi-component alloys with FCC crystal structure. The first article was published in the *Intermetallics* in 2014; the second article was submitted to *Acta Materialia* on June 25th 2014; and the third article is under preparation for submission to Scripta Materialia. In keeping with the guidelines for a multi-part dissertation by the Graduate School of the University of Tennessee, each article is presented as an individual chapter in the dissertation, with the figures and tables are listed in an appendix at the end of each chapter.

Traditional design and development of alloys is mainly based on one principle element, such as iron in steels [e.g., 1-3], copper in brasses and bronzes [e.g., 4-5], aluminum in aluminum alloys [e.g., 6-9], nickel in superalloys [e.g., 10-13], and titanium in Ti-based alloys [e.g., 14-16], leading to an enormous amount of knowledge about alloys whose compositions are located at the edges or the corners of the phase diagrams. Compared to these, there is very little knowledge about alloys containing several main components at or near equiatomic compositions. Motivated by this, Yeh et al. [17] tried a new approach to alloy design including multiple (five or more) principle elements at or near equiatomic at or near equiatomic ratios and defined this class of alloys as "high entropy (HE) alloys". In general, from physical metallurgy intuition, increasing number of additive elements will simultaneously increase the probability that second phases will

precipitate out. Recently, however, a limited number of alloys containing multiple constituent elements in equiatomic or near-equiatomic concentrations have been discovered and shown to crystallize as solid solutions with simple (FCC or BCC) crystal structures [18-21]. The striking feature of some of these alloys is that they are comprised of elements with very different crystal structures, which contradicts traditional notions of solid solubility based on empirical observaions such as Hume-Rothery rules. As a possible explanation for this, it has been hypothesized that their remarkable solid solubility is the result of high configurational entropy. High configurational entropies are expected to be able to overcome enthalpies of compound formation and phase separation, thereby stabilizing the solid-solution state relative to the various possible multiphase states in such highly alloyed materials. This high-entropy concept, if generally valid, provides new ways to rationalize alloy phase stability. Other than the high entropy effect, sluggish diffusion [22], severe lattice distortion [17] and large solid solution strengthening [17] are also expected and have been shown to be important effects for the high entropy alloys. Motivated by these anticipations and earlier observations, tremendous amount of efforts have been put mounted during the past decade the investigation and exploration of various properties of high entropy alloys. High strength, outstanding wear resistance, exceptional high-temperature strength, good structural stability, good corrosion and oxidation resistance have been observed for some HE alloys, however, the deformation mechanisms of HE alloys are not well understood.

Recently, an equiatomic quinary alloy, FeNiCoCrMn, was fabricated and shown to be FCC-structured single phase solid solution alloy [18]. Since its discovery, extensive research has been conducted, including its recrystallization behavior [23] and diffusion kinetics [21]. More importantly, to understand its deformatio, the mechanical properties of this alloy were

investigated as a function of temperature by Gali et al. [24] and Otto et al [25]. A striking feature observed in the behavior of this alloy is that both its strength (yield strength and ultimate tensile strength (UTS)) and elongation increase with the decreasing of temperature. Through microstructural characterization, the increase of UTS and elongation at low temperature (77 K) were attributed to the transition of deformation mode from dislocation-mediated plasticity to nano-twinning. Regarding the yield strength, it has been shown and widely accepted that the yield strength of BCC metals is highly temperature-dependent [26]. In general there are two barriers that contribute the temperature-dependence of yield strength of BCC metals [27]. The first one is the locking of dislocations by interstitial solute atoms, and the second is the Peierls-Nabarro barrier. Because of the difficulty of reducing interstitial impurities to levels where they would be only sparsely distributed along dislocations, it is not possible to distinguish with any certainty between these two possibilities. However, earlier work with highly purified iron showed that the yield strength is very low when the impurities reach extremely low levels, but there is still a substantial temperature dependence which must arise from the Peierls-Nabarro barrier [28]. Due to a much smaller Peierls-Nabarro barrier, the yield strength of pure FCC metals has been observed to be relatively insensitive to changes in temperature (at low homogeneous temperatures), as confirmed experimentally [26]. However, similar to what has been observed in the FeNiCoCrMn alloy, a temperature-dependent yield strength has been reported for several binary FCC solid solution alloys [29-36]. In these materials, the yield strength is normally separated into athermal and thermal portions, with the former arising from the interactions of a dislocation with long-range obstacles and the latter from the interaction of a dislocation and short-range barriers. Both the athermal and thermal portions were observed to increase with the solute concentrations, indicating an increase of the amount of both types of

obstacles. However, for the binary FCC solutions and for the equiatomic quinary alloy, FeNiCoCrMn, a fundamental understanding of the responsible mechanisms and the nature of the obstacles which contribute to the temperature sensitivity remains elusive.

To develop better theories of unusual temperature sensitivities of mechanical properties of equiatomic multi-component alloys, it is important to experimentally characterize the mechanical behavior of a range of equiatomic solid solution alloys as a function of temperature. To this end, we will investigate in this dissertation a family of equiatomic binary, ternary and quaternary alloys which are all subsets of the "parent" FeNiCoCrMn alloy. The first step is to examine all available phase diagrams for these alloys. Phase diagrams for quaternaries are virtually non-existent; thus we have to experimentally determine the stability. For ternary and binary alloys, phase diagrams are helpful for excluding the alloys that will not be able to solidify as FCC solid solutions. The remaining alloys which will possibly be FCC solid solutions have been drop-cast and homogenized to identify their phase components. For the alloys that have been identified as FCC solid solutions, thermomechanical processing is conducted to investigate their phase stability and recovery, recrystallization and grain growth behavior. This first part is covered in the first published article "Recovery, Recrystallization, Grain Growth and Phase Stability of a Family of FCC-Structured Multi-Component Equiatomic Solid Solution Alloys". After this, the mechanical properties of the identified FCC solid solutions are investigated as a function of temperature. To achieve this, alloys with comparable grain size are tensile tested under five different temperatures (77-673 K) at a constant strain rate (10^{-3} s^{-1}). Their melting temperatures, shear moduli and Poisson's ratios are measured to help us understand and analyze data. The experimental observations and mechanistic understanding of the mechanical properties the equiatomic alloys is covered in the second submitted article "Temperature Dependence of the

Mechanical Properties of Equiatomic Solid Solution Alloys with FCC Crystal Structures". From this set of experimental data, another effect is observed, an alloying arising from the addition of different elements. A statistical method is used to help understand this and analyze this which is covered in the third article "Alloying Effects on the Mechanical Properties of Equiatomic FCC Solid Solution Alloys".

References

[1] Hall EO. Proceedings of the Physical Society of London Section B 1951; 64(381): 747.

[2] Bhadeshia H, Edmonds DV. Metallurgical Transactions A-Physical Metallurgy and Materials Science 1979; 10: 895.

[3] Chen X, Stubbins JF, Hosemann P at al. Journal of Nuclear Materials 2010; 398(1): 172.

[4] Sharififar M, Mousavi S, Akbari, AA. Mater Sci En A 2014; 594: 118.

[5] Ardley GW, Cottrell AH. Proceeding of the Royal Society of London A 1953; 219: 328.

[6] Wu ZG, Song M, He YH. Mater Sci En A 2009; 504: 183.

[7] Hahn GT, Rosenfield AR. Metallurgical Transactions A 1975; 6(4): 653.

[8] Song M, Wu Z, He Y. Mater Sci En A 2008; 497: 519.

[9] Christman T, Suresh S. Acta Metallurgica 1988; 36(7): 1691.

[10] Chen X, Yang Z, Sokolov MA et al. Mater Sci En A 2013; 563: 152

[11] Giamei AF, Anton DL. Metallurgical Transactions A 1985; 16(11): 1997.

[12] Chen X, Sokolov MA, Sham S et al. Journal of Nuclear Materials 2013; 432(1): 94.

[13] Choe H, Dunand DC. Acta Materialia 2004; 52(5): 1283.

[14] Sun P, Fang ZZ, Koopman M. Adv Eng Mater 2013; 15(10): 1007.

[15] Fang ZZ, Sun P. Key Eng Mater 2012; 520: 15.

[16] Fang ZZ, Sun P, Wang H. Adv Eng Mater 2013; 14(6): 383.

[17] Yeh JW, Chen SK, Lin SJ, et al. Adv Eng Mater 2004; 6: 299.

[18] Cantor B, Chang ITH, Knight P, et al. Mater Sci Eng A 2004; 375-377: 213.

[19] Senkov ON, Scott JM, Senkova SV, et al. J Alloys Compd 2011; 509: 6043.

[20] Senkov ON, Wilks GB, Miracle DB, et al. Intermetallics 2010; 18: 1758.

[21] Senkov ON , Wilks GB, Scott JM, et al. Intermetallics 2011; 19:698.

[22] Tsai KY, Tsai MH, Yeh JW. Acta Mater 2013; 61:4887.

[23] Liu WH, Wu Y, He JY, et al. Scripta Mater 2013; 68: 526.

[24] Gali A, George EP. Intermetallics 2013; 39:74.

[25] Otto F, Dlouhy A, Somsen Ch, et al. Acta Mater 2013; 61: 5743

[26] Low JR. Behavior of Metals at LowTemperatures. ASM 1952.

[27] Honeycombe RWK. The Plastic Deformation of Metals. ASM 1975.

[28] Hutchison MM. Philo Mag 1963; 8: 121

[29] Schwink CH, Wille TH. Scripta Metall 1980; 14: 1093.

[30] Demirskiy VV, Komnik SN, Starstsev VI. Phys. Met. Metall 1979; 46: 151.

[31] Suzuki H. in: McQqueen HJ, Bailon JP, Dickson JJ, et al. Strength of Metals and Alloys, Pergamon Press, 1985, 3: 1727.

[32] Koppenaal TJ, Fine ME. Trans AIME 1962; 224: 347.

[33] Kamada K, Yoshizawa I. J. Phys. Soc. Jpn 1971; 31(4): 1056.

[34] Traub H, Neuhauser H, Schwink CH; Acta Met 1977; 25: 437.

[35] Feltham P, Copley GJ. Acta Metall 1960; 8: 542.

[36] Butt MZ, Ghauri IM. Phys. Stat. Sol (a) 1988; 107: 187.

CHAPTER I

Recovery, Recrystallization, Grain Growth and Phase Stability of a Family of FCC-Structured Multi-Component Equiatomic Solid Solution Alloys

A version of this chapter was originally published by Z. Wu, H. Bei, F. Otto, G.M. Pharr, E.P. George in 2014:

Z. Wu, H. Bei, F. Otto, G.M. Pharr, E.P. George. Recrystallization, Grain Growth and Phase Stability of a Family of FCC-Structured Multi-Component Equiatomic Solid Solution Alloys. Intermetallics 2014; 46:131-140.

Authors:

Z. Wu

Materials Science and Engineering Department, University of Tennessee, Knoxville, TN 37996, USA

H. Bei

Materials Science and Technology Division, Oak Ridge National Laboratory, Oak Ridge, TN 37831, USA

F. Otto, G.M. Pharr, E.P. George

Materials Science and Engineering Department, University of Tennessee, Knoxville, TN 37996, USA; and Materials Science and Technology Division, Oak Ridge National Laboratory, Oak Ridge, TN 37831, USA

Z. Wu's involvement in the article: designed experimental procedures, prepared the samples, performed thermo-mechanical treatments and microstruatural characterizations, analyzed the experimental data, wrote and revised the article.

Co-researchers' contributions are listed as follows:

H. Bei helped Zhenggang with the designation and operation of experimental procedures and the discussion of data and revised the article.

F. Otto provides samples, discussed the experiment data with Zhenggang and revised the article.

G.M. Pharr, E.P. George provided research guidelines and worked with Zhenggang to analyze the experimental data and revised the article.

Abstract

The equiatomic high-entropy alloy FeNiCoCrMn is known to crystallize as a single phase with the face-centered cubic (FCC) crystal structure. To better understand this quinary solid solution alloy, we investigate various binary, ternary and quaternary alloys made from its constituent elements. Our goals are twofold: (*i*) to investigate which of these lower order systems also form solid solution alloys consisting of a single FCC phase, and (*ii*) to characterize their phase stability and recovery, recrystallization, and grain growth behaviors. X-ray diffraction (XRD) and scanning electron microscopy with backscattered electron images showed that three of the five possible quaternaries (FeNiCoCr, FeNiCoMn and NiCoCrMn), five of the ten possible ternaries (FeNiCo, FeNiCr, FeNiMn, NiCoCr, and NiCoMn), and two of the ten possible binaries (FeNi and NiCo) were single-phase FCC solid solutions in the cast and homogenized condition, whereas the others either had different crystal structures or were multi-phase. The single-phase FCC quaternary, FeNiCoCr, along with its equiatomic ternary and binary subsidiaries, were selected for further investigations of phase stability and the thermomechanical processing needed to obtain equiaxed grain structures. Only four of these subsidiary alloys—two binaries (FeNi and NiCo) and two ternaries (FeNiCo and NiCoCr)—were found to be single-phase FCC after rolling at room temperature followed by annealing for 1 h at temperatures of 300-1100 °C. Pure Ni, which is FCC and one of the constituents of the quinary high-entropy alloy (FeNiCoCrMn), was also investigated for comparison with the higher order alloys. Among the materials investigated after thermomechanical processing (FeNiCoCr, FeNiCo, NiCoCr, FeNi, NiCo, and Ni), FeNiCo and Ni showed abnormal grain growth at relatively low annealing temperatures, while the other four showed normal grain growth behavior. The grain growth exponents for all five of the equiatomic alloys were found to be ~0.25 (compared to ~0.5 for unalloyed Ni), suggesting that solute drag may control grain growth in the alloys. For all five alloys, as well as for pure Ni,

microhardness increases as the grain size decreases in a Hall-Petch type way. The ternary alloy NiCoCr was the hardest of the alloys investigated in this study, even when compared to the quaternary FeNiCoCr alloy. This suggests that solute hardening in equiatomic alloys depends not just on the number of alloying elements but also their type.

1. Introduction

High-entropy (HE) alloys were defined by Yeh et al. [1] as equiatomic or near-equiatomic alloys containing at least five principal elements. Their work was an attempt to rationalize why certain relatively concentrated multi-element alloys solidify as simple (BCC or FCC) solid solutions rather than with multi-phase microstructures consisting of several different intermetallic compounds—as would be the expectation from physical metallurgy intuition. Yeh et al. hypothesized that the high configurational entropies of equiatomic alloys containing five or more elements would overwhelm the enthalpies of compound formation, thereby suppressing intermetallic formation and favoring the formation of solid solutions. Consistent with such a hypothesis, it has been found that the microstructures of some HE alloys are in fact single-phase FCC [2, 3] or BCC [4, 5]. However, most alloys that are referred to in the literature as high-entropy alloys actually contain secondary phases [e.g., 6-8]. In such multi-phase alloys, the configurational entropy should be much lower [9] than that of a random mixture assumed by Yeh et al. [1] and thus unlikely to be able to overcome the effects of the enthalpies of compound formation and phase separation [9]. Nevertheless, the term “high-entropy alloys” has taken hold in the literature and is now used to describe all equi- or near equi-atomic multi-component alloys containing five or more elements regardless of whether they are true single-phase solid solutions or not.

Due to the multiple alloying elements present in HE alloys, they are expected to exhibit a high degree of solid solution hardening [1]. This has led to numerous research efforts aimed at finding alloys with simple microstructures and promising mechanical properties [e.g., 2, 5, 10-14]. A prominent example is the equiatomic FeNiCoCrMn alloy that was first reported by Cantor et al. [2] to solidify as a single-phase solid solution. Subsequent studies showed that it exhibits a high

degree of thermodynamic stability [9], that it has excellent malleability [12], and that its grain size can be controlled by rolling and recrystallization [12-14]. Gali and George [12] first reported and Otto et al. [14] further investigated the tensile properties of this high-entropy alloy, which shows a strong increase in strength with decreasing temperature accompanied by a large increase in ductility [12, 14]. Through microstructural characterization by transmission and scanning electron microscopy, the increases in ultimate tensile strength and ductility at liquid nitrogen temperature were attributed to a changeover in deformation mechanism from dislocation mediated plasticity to nano-twinning [14]. In contrast, the mechanism responsible for the strong increase in yield strength with decreasing temperature [12, 14], which is atypical for pure FCC metals [e.g., 15] but observed in binary FCC solid solutions [e.g., 16-18], is not well understood.

To better understand the mechanical behavior of this HE alloy (FeNiCoCrMn) and the effects of the number/type of alloying elements on mechanical properties and phase stability, it is important to systematically study its various equiatomic subsystems, namely the five quaternary, ten ternary, and ten binary alloys that can be formed from the constituent elements of the HE quinary, as shown in Fig. 1.1. To this end, we arc melted and homogenized these sub-alloys and identified the phases present in their microstructures. Of the five quaternaries, three were found to be single-phase FCC, and from those we selected for further study the quaternary alloy FeNiCoCr and its equiatomic ternary and binary subsets. Our rationale for this selection was that: (*i*) the FeNiCoCr alloy has been reported to exhibit mechanical properties similar to the high-entropy FeNiCoCrMn alloy [12], and (*ii*) many high-entropy alloys investigated in the literature are based on the FeNiCoCr equiatomic composition to which additional elements such as Al [19], Cu [20], Mn [9, 12-14], Ti, Nb, and Mo [21] are added. We also investigated pure (unalloyed) Ni to obtain a baseline against which the higher order solid solution alloys can be compared. For

each of these materials, we investigated phase stability, microstructure and microhardness evolution as a function of heat treatment after cold rolling.

2. Methods and Experimental Procedures

2.1. Phase Diagram Assessments

Quaternary phase diagrams are virtually nonexistent in the literature. Therefore, we had no choice but to experimentally identify the phases present in our equiatomic quaternaries. In contrast, ternary and binary phase diagrams tend to be more common so we used them as a first step in our analysis followed by experimental verification of the phases that were actually present. All phase diagrams used in this study were taken from the ASM Alloy Phase Diagram Database [22]. The data gathered from the available phase diagrams are summarized in Table 1.1 where the phases present at various temperatures are listed. Based on these data, the equiatomic alloys FeCoCr, FeCrMn, FeCr, NiCr, CoCr and CrMn were eliminated from further consideration since they have either the BCC crystal structure or consist of multiple phases at high temperatures. In the case of Fe-Co alloys, the FCC phase is stable only above 985 °C; at lower temperatures, either BCC or B2 is the stable phase. Additionally, phase separation has been shown to occur in a surface layer up to 70 μm in thickness (not associated with surface oxidation) at temperatures to 1300 °C [23] including at the FeCo equiatomic composition [24]. Therefore, it, too, was excluded from further study since our focus was on those alloys that are single-phase FCC at room temperature. The remaining eight ternary and five binary equiatomic alloys could *potentially* form single-phase FCC solid solutions, but experimental validation was necessary since phase diagrams were either not available (in some cases), or available only for a

limited range of temperatures. Of the five elements in the quinary alloy (FeNiCoCrMn), only Ni has the FCC crystal structure at room temperature. Based on these starting observations, several different ingots were prepared and analyzed for experimental verification of phase stability as described below.

2.2. Alloy Preparation and Characterization

Ingots of the selected equiatomic quaternaries, ternaries, binaries, and pure Ni were produced by arc melting the constituent elements (>99.9% pure) in a water-cooled copper hearth under argon atmosphere. Since Mn oxidizes easily, it was cleaned in a 25% nitric acid solution immediately before use; additionally, since it has a high vapor pressure, it was stacked between the other constituents to minimize evaporation. Even so, there was some loss of Mn during melting, and extra Mn was added to the charge to compensate for its weight loss based on our previous experience with Mn-containing HE alloys [9, 12, 14]. To improve compositional homogeneity, the arc-melted buttons were flippedand re-melted five times before drop casting into square cross-section copper molds measuring 12.7 mm $\times$ 12.7 mm $\times$ 127 mm.

The drop-cast ingots were homogenized for 24 h at different temperatures, as shown in Table 1.1, followed by water quenching. Homogenization was performed at as high a temperature as possible without resulting in melting. After homogenization, crystal structures were examined by x-ray diffraction with Cu-target radiation at 40 kV and 40 mA on 2.54-mm thick slices. The samples were scanned through 2θ ranging from 20 to 90 degrees with a scan rate of 1.2 degrees/minute. Microstructures were imaged in a JEOL 6500 FEG scanning electron microscope (SEM) operated in the backscattered electron (BSE) mode.

For the alloys selected for further studies of phase stability, recovery, recrystallization and grain growth, additional ingots measuring 12.7 mm × 25.4 mm × 127 mm were cast. The solidus temperatures of these solid solution alloys were measured using a NETZSCH 404 C differential scanning calorimeter (DSC). In this paper, the solidus temperatures are defined as the start temperature of the endothermic peaks observed on the DSC traces upon heating from room temperature to the melting temperature. The homogenized ingots were rolled at room temperature in steps from 12.7 mm to 1 mm (total thickness reduction of 92%) without cross-rolling or intermediate annealing. Specimens were then cut perpendicular to the rolling direction and annealed at temperatures between 300 and 1100 °C. After annealing, crystal structures and microstructures were analyzed as described previously.

Grain growth kinetics were investigated at 900 °C and annealing times of 1, 2, 4, 8, and 16 h. Pure Ni was excluded from the grain growth study because its starting grain size after 1 h was very large (~130 µm) and was expected to grow to a significant fraction of the thickness of the rolled sheets (~1000 µm) after longer annealing times. Grain size measurements were made on SEM BSE images of the alloy microstructures using the linear intercept method; at least 150 grains were counted for each specimen.

Microhardness was measured with a LECO LM 100_{AT} Vickers Hardness tester using a load of 500 g. Ten indents were made for each condition from which average values of hardness and standard deviations were calculated.

3. Results and Discussion

3.1. Phase Identification and Phase Stability

X-ray diffraction patterns and BSE images of the cast and homogenized alloys are shown in Figs. 1.2-1.4. Three of the five quaternaries, FeNiCoCr, FeNiCoMn and NiCoCrMn, five of the eight ternaries, FeNiCo, FeNiCr, FeNiMn, NiCoCr and NiCoMn, and two of the five binaries, FeNi and NiCo, exhibited only FCC peaks, while the XRD spectra of the others included peaks from other phase(s). The BSE micrographs shown for each alloy are consistent with their respective XRD patterns. In the case of FeCoMn, FeMn, NiMn, and CoMn, phase diagrams show that only an FCC phase should be present in these alloys at high temperatures (Table 1.1). However, their microstructures after homogenization and water quenching are not single-phase (Figs. 1.3 and 1.4) indicating that the high-temperature FCC phase is not stable at low temperatures. Figure 1.1 summarizes the above observations and identifies in red those materials that are single-phase FCC at room temperature after casting and homogenization. Starting from the quinary FCC-structured equiatomic alloy (FeNiCoCrMn), there are three quaternary, five ternary, and two binary equiatomic alloys that solidify as single-phase FCC solid solutions. Possible criteria for why some high-entropy alloys tend to solidify as a single-phase FCC solid solution while others tend to solidify as multiphase were proposed by Guo et al., including valence electron concentration (VEC) [25] and lattice distortion [26]. According to Guo et al. [25], when the effective VEC of an alloy is ≥ 8, it tends to form as single-phase FCC, for values between 6.87 and 8, it tends to form as two-phase FCC-BCC, and for values ≤ 6.67, it tends to form as single-phase BCC. To determine whether this was true in our equiatomic binaries, ternaries and quaternaries, we calculated their effective VECs using the elemental VECs given in [25]. We found that, except for two binaries (FeCo and NiMn), our alloys generally obeyed the

VEC criterion of Guo et al. [25]. Their second criterion, based on lattice distortion [26], requires knowledge of the lattice parameters of our alloys, which is beyond the scope of the current study and can be taken up in a follow-on investigation. From these, we selected the FeNiCoCr quanternary and its ternary and binary subsets for further investigation.

Figure 1.5 shows XRD patterns and BSE images obtained from FeNiCoCr, FeNiCo, FeNiCr, NiCoCr, FeNi, and NiCo after cold rolling and annealing at 800 °C for 1 hour. All of these alloys still exhibit only FCC peaks, except for the FeNiCr alloy, which exhibits additional peaks belonging to another phase. This second phase, which is present mainly on the grain boundaries, has the BCC structure based on our analysis of its XRD pattern and ternary phase diagram. Therefore, the FeNiCr alloy was excluded from further consideration since our focus here is on those alloys that are single-phase FCC after thermomechanical processing. The remainder of this paper deals with those materials (FeNiCoCr, FeNiCo, NiCoCr, FeNi, NiCo,and Ni) that were single-phase FCC after cold rolling and annealing for 1 h at temperatures of 300-1100 °C, as determined by XRD and microstructural analyses in a SEM. It is possible that some of these alloys (e.g., FeNi) might decompose into intermetallic phases if subjected to long-term, low-temperature anneals.

3.2. Microstructural Evolution during Casting, Homogenization, Cold Rolling and Annealing

Figure 1.6 shows representative microstructures of the equiatomic FeNiCoCr alloy in the cast, homogenized, and recrystallized states. The as-cast specimen consists of large elongated grains extending from the edges to the center of the rectangular cross-section molds (Fig. 1.6a),

consistent with the heat flow directions during solidification. After homogenization at 1200 °C for 24 h, the elongated grains near the center of the casting are replaced by more equiaxed grains (Fig. 1.6b). After cold rolling and annealing at 900 °C, the microstructure is fully recrystallized and comprised of equiaxed grains (Fig. 1.6c). A similar microstructural evolution was observed in the other alloys. Figure 1.7 shows the recrystallized microstructures of all the equiatomic alloys investigated here, along with that of pure Ni, after cold rolling and annealing at 1000 °C for 1 hour. All of them exhibit equiaxed grains, but with different grain sizes and different numbers of annealing twins.

3.3. Recovery, Recrystallization and Grain Growth Kinetics

Microhardnesses after 1-h anneals at various temperatures are shown in Fig. 1.8a. The open arrows indicate the start of recrystallization and the filled arrows the completion of recrystallization (T_i and T_f are the corresponding temperatures at which recrystallization starts and finishes, respectively). Note that T_i and T_f are only approximate since our annealing temperatures had an increment of 100 °C. Figure 1.8 also includes, as representative examples, BSE images of the microstructures of the FeNiCo alloy: when annealed at 500 °C (below T_i), it exhibits a fully wrough tmicrostructure (Fig. 1.8b); when annealed at 600 °C (T_i), it exhibits a partially recrystallized microstructure (Fig. 1.8c); and when annealed at 800 °C (T_f), it exhibits a fully recrystallized microstructure (Fig. 1.8d). The overall decrease in hardness with increasing temperature (Fig. 1.8a) is presumably the combined result of recovery, recrystallization and grain growth. A determination of the relative contributions of each of these processes to the hardness decrease would require more detailed analyses at finer temperature increments.

As would be expected based on solute effects on strength, the smallest hardnesses were observed in pure nickel with the binaries having measurably higher hardnesses. However, the hardest material was not the quaternary but one of the ternaries (NiCoCr), indicating that the nature of the alloying elements has to be taken into account in addition to the sheer number of alloying elements.

Table 1.2 presents the temperatures at which melting commenced in the alloys, i.e., the solidus temperatures, based on the DSC measurements. For all the alloys shown in Fig. 1.8a, the solidus temperatures lie in a relatively narrow range (1417-1462 °C). Therefore, the hardness differences seen in Fig. 1.8a (related to the different temperature ranges for recovery, recrystallization and grain growth) are not due to differences in the homologous temperatures. Rather, they appear to be related to the nature of the specific elements present in the different alloys.

Traditional notions of the effects of solutes on recovery, recrystallization and grain growth behavior can help us understand the differences seen in Fig. 1.8, even though, in equiatomic alloys, unlike in more dilute solid solutions, there is no "solvent" into which solute atoms are added. Solute atoms can influence the stacking fault energy and/or impede the movement of dislocations [27]. Stacking fault energy (γ_{SFE}) is one of the most important parameters that determines the degree of recovery by affecting the extent to which dislocations dissociate, which in turn determines the rate of dislocation climb and cross slip, which are the mechanisms that usually control the rate of recovery [27]. In metals with low γ_{SFE} such as copper**,** climb is difficult, which slows down recovery [28]. On the other hand, in metals with high γ_{SFE} such as aluminum**,** climb is rapid, and the rate of recovery tends to be higher [e.g., 29, 30]. It has been shown that additions of Cr, Co, and Fe all lower the stacking fault energy of Ni, with iron having the smallest effect and Cr the largest [31,32]. Based on these results, one might expect the

stacking fault energies of our materials to increase in the order: NiCoCr < FeNiCoCr < NiCo < FeNiCo < FeNi < Ni. The annealed microstructures shown in Fig. 1.7, with different densities of annealing twins, are consistent with this trend of stacking fault energies. Thus, the relatively rapid decrease in the hardness of pure Ni can be attributed to its higher stacking fault energy while the slower decrease in some of the equiatomic alloys may be due to their lower stacking fault energies. Our experimental results are consistent with the work of Seymour and Harker [33], who found that there was no hardness reduction in the FeNi equiatomic alloy after a 1-h anneal at 500 °C but significant reduction after a 1-h anneal at 600 °C.

Figure 1.8 also shows that the recrystallization start (T_i) and finish (T_f) temperatures depend on alloy composition. NiCo and Ni have similar T_i and T_f temperatures, which are significantly lower than those of FeNiCoCr, FeNiCo, NiCoCr and FeNi. Recrystallization temperatures usually vary inversely with the degree of cold work [e.g., 34, 35]. In the present study, all the materials investigated were subjected to the same degree of cold rolling (92% reduction in thickness); yet, as shown in Fig. 1.8, they exhibited significantly different recrystallization temperatures. Thus, once again the specific nature of the alloying elements appears to be important.

Figure 1.9 shows the mean grain size after 1-h anneals at various temperatures. With the exception that pure Ni exhibited both the largest grain size and the greatest amount of grain growth with annealing, there are no general trends in the observed behavior as a function of the number of elements in the alloy. The NiCoCr alloy had the smallest grain size at all annealing temperatures.

Two of the alloys exhibited abnormal grain growth - pure Ni between 500 and 700 °C and FeNiCo at 800 °C. The short arrows in Fig. 1.9 point to the annealing temperatures at which abnormal grain growth was observed. An example of abnormal grain growth in pure Ni annealed at 500 °C for 1 h is shown in the inset BSE image in Fig. 1.9, which shows the presence of a few large grains in a matrix of much smaller grains. All the other alloys showed normal grain growth at all temperatures, with a relatively narrow grain size distribution that evolved in a uniform fashion. Abnormal grain growth in alloys has been attributed to texture [36, 37] or grain boundary pinning by precipitates [38] and can usually develop if certain boundaries are pinned more than others [39]. In high-purity bulk polycrystals and in specimens without texture, the occurrence of abnormal grain growth has been attributed to the segregation of impurity or solute atoms at grain boundaries [40-44]. Randle and Horton [45] observed anomalous grain growth in high-purity Ni for annealing temperatures lower than $0.68T_m$ but relatively normal grain growth for higher temperature anneals. They attributed this to grain boundary structural transformations, which can lead to a change in the mobility of some grains boundaries and allow them to migrate at a faster rate than average. Lee et al. [46] further linked abnormal grain growth in pure Ni to the formation of faceted grain boundaries. Additional investigations are needed to determine whether any of these factors are responsible for the abnormal grain growth seen here in Ni and FeNiCo.

The kinetics of grain growth are often analyzed according to the rate equation:

$$d^{\frac{1}{n}} - d_o^{\frac{1}{n}} = kt, \quad (1)$$

where d is the average grain size after annealing for time t, d_o is the average initial grain size, k is the rate constant and n is the grain growth exponent [47, 48]. When d_o is very small and a

significant amount of grain growth has occurred (i.e., $d>>d_o$), this expression can be simplified and written in its more usual form [49]

$$d^{\frac{1}{n}} = kt, \tag{2}$$

Burke and Turnbull [50] obtained a theoretical value of n = 0.5 for the grain growth exponent, but many experimental studies have reported that n is generally well below this value and that it varies with composition and temperature [27]. In fact, a grain growth exponent of 0.5 has rarely been found even in pure metals with very low impurity levels [27]. In our case, all the equiatomic alloys have a grain growth exponent close to 0.25 (Fig. 1.10), which is at the lower end of typical values reported in earlier studies on zone-refined metals where the n values ranged from 0.25 to 0.5 [27]. To eliminate from consideration the very early stages of recrystallization and grain growth, the 1-hour grain size data, although shown in Fig. 1.10, were not considered in our estimation of the grain growth exponents. Values of n less than 0.5 are often attributed to solute drag effects on the boundary mobility [51, 52]. In the case of unalloyed Ni, a grain growth exponent close to 0.5 has in fact been reported [45].

3.4. Microhardness Dependence on Grain Size

Figure 1.11 shows the dependence of microhardness on mean grain size for the equiatomic alloys and pure Ni. The data indicate that the hardnesses all follow a Hall-Petch type relationship. As a consequence, the data in Fig. 1.11 can be fit to the expression

$$H = H_o + k_H d^{-1/2}, \tag{3}$$

where H is the hardness at a grain size d, H_o is the hardness intercept at $d^{-1/2}=0$, and k_H, the Hall-Petch slope, is a material parameter related to the grain boundary strength.

Table 1.3 lists the Hall-Petch constants for the different alloys. In general, the Hall-Petch slopes follow the expected stacking fault energy trends discussed earlier. Fischmeister and Karlsson [53] noted that an increase in the value of the stacking fault energy decreases the Hall-Petch slope and attributed this effect to the easy formation of a cell structure, reasoning that cell boundaries, rather than grain boundaries, limit the slip lengths of dislocations in such cases. However, it is certainly possible that other factors control the behavior in these complex alloys.

At a given grain size, the hardness differences in Fig. 1.11 are a measure of the hardening effects of different solutes. Due to the large number of alloying elements in HE alloys, a high degree of solid solution hardening has been hypothesized in equiatomic multi-component alloys [1]. However, our results show that simply increasing the number of alloying elements does not always make the materials harder. For example, the addition of Co to pure Ni to form a binary, or to the FeNi alloy to produce a ternary, causes only minor hardening while the addition of Cr to NiCo and FeNiCo causes tremendous hardening. In other words, the nature of the added element also plays an important role in the hardening of equiatomic alloys. In general, the factors that affect solid solution hardening are size misfit, modulus mismatch, stacking fault energy changes, and long-range and/or short-range ordering. The magnitude of the elastic interaction force between a dislocation and a solute increases with both the atomic size and modulus misfits between solute and solvent atoms. In terms of the Seitz radii, the atomic sizes of Fe, Ni, Co, and Cr are 1.411, 1.377, 1.385, and 1.423 Å, respectively [54]. The largest difference in these atomic sizes is only 3.3% suggesting that the difference in the hardness of the alloys is unlikely to be due to size misfits. In contrast, the Young's moduli of Fe, Ni, Co and Cr are 211, 200, 209, and

279 GPa, respectively [55], with the largest difference yielding a misfit 39.5% between Cr and Ni. Therefore, the observed hardening effects might be largely due to the modulus mismatch between Cr and the other elements, although it is difficult to extrapolate the general principles governing strength beyond the binary alloys.

4. Summary and Conclusions

The high-entropy alloy FeNiCoCrMn has previously been shown to be single-phase FCC. All possible equiatomic subsystems (quaternary, ternary, and binary) of this quinary alloy were studied by assessing their available phase diagrams and experimentally verifying which of the sub-alloys formed single-phase FCC solid solutions. One of the single-phase quaternaries, FeNiCoCr, plus its equiatomic ternary and binary subsets that had the FCC crystal structure, were then selected for further investigations of phase stability, recovery, recrystallization and grain growth behavior. Pure Ni was also investigated to provide a baseline against which to compare the alloys. It was shown that neither the ability to form a single-phase solid solution, nor the degree of solid solution hardening, was determined solely by the *number* of alloying elements; rather the *type* of elements present in the alloys needs to be taken into account. Based on this study, the following conclusions can be drawn:

(1) Three quaternaries, FeNiCoCr, FeNiCoMn, and NiCoCrMn, five ternaries, FeNiCo, FeNiCr, FeNiMn, NiCoCr, and NiCoMn, and two binaries, FeNi and NiCo, are single-phase FCC solid solutionsin the cast and homogenized condition.

(2) Among the FCC subsets of the FeNiCoCr alloy, phase separation occurs in one alloy, FeNiCr, when it is cold rolled and annealed (recrystallized), while all the others remain as single-phase FCC solid solutions.

(3) FeNiCo and Ni exhibit abnormal grain growth at relatively low annealing temperatures while all the other alloys show normal grain growth behavior.

(4) The grain growth exponents of the equiatomic alloys FeNiCoCr, FeNiCo, NiCoCr, FeNi, and NiCo are ~0.25, compared to ~0.5 for pure Ni, suggesting that solute drag may alter the grain growth kinetics of the equiatomic alloys.

(5) All the equiatomic alloys as well as pure Ni show a Hall-Petch type of grain size dependence of microhardness.

(6) The ternary equiatomic alloy NiCoCr is harder than all the other alloys, including the quaternary alloy FeNiCoCr, suggesting that solid solution hardening in multi-component equiatomic alloys cannot be solely determined by the number of alloying elements; the type of alloying elements is also important.

Acknowledgments: This research was supported by the U.S. Department of Energy, Office of Basic Energy Sciences, Materials Sciences and Engineering Division. FO also received funding from the Alexander von Humboldt Foundation through a Feodor Lynen Research Fellowship.

References

[1] Yeh JW, Chen SK, Lin SJ, et al. Adv Eng Mater 2004; 6: 299

[2] Cantor B, Chang ITH, Knight P, et al. Mater Sci Eng A 2004; 375-377: 213

[3] Lucas MS, Wilks GB, Mauger L, et al. Appl Phys Lett 2012; 100: 251907.

[4] Senkov ON, Wilks GB, Scott JM, et al. Intermetallics 2011;19:698

[5] Senkov ON, Scott JM, Senkova SV, et al. J Alloys Compd 2011; 509: 6043

[6] Wang XF, Zhang Y, Qiao Y, et al. Intermetallics 2007; 15: 357

[7] Guo S, Ng C, Liu CT. J Alloys Compd 2013; 557: 77

[8] Zhu JM, Fu HM, Zhang HF, et al. Mater Sci Eng A 2010; 527: 6975

[9] Otto F, Yang Y, Bei H, et al. Acta Mater 2013; 61(7): 2628

[10] Senkov ON, Wilks GB, Miracle DB, et al. Intermetallics 2010; 18: 1875

[11] Zhou YJ, Zhang Y, Wang YL, et al. Appl Phys Lett 2007; 90: 1819

[12] Gali A, George EP. Intermetallics 2013; 39:74

[13] Liu WH, Wu Y, He JY, et al. Scripta Mater 2013; 68: 526

[14] Otto F, Dlouhy A, Somsen Ch, et al. Acta Mater 2013; 61: 5743

[15] Low JR. Behavior of Metals at LowTemperatures. ASM. 1952, p48

[16] Wille TH, Schwink CH. Acta Metall 1986; 34: 1059

[17] H. Suzuki, in: P.O. Kettunen, T.K. Lepisto, M.E. Lehtonen (Eds.), Strength of Metals and Alloys (ICSMA 8), Pergamon Press, Oxford, 1988; 2: 573

[18] Traub H, Neuhauser H, Schwink CH. Acta Metall 1977; 25: 437

[19] Lin CM, Tsai HL. Intermetallics 2011; 19: 288

[20] Praveen S, Murty BS, Kottada RS. Mater Sci Eng A 2012; 534: 83

[21] Bei H. US Patent 2013/0108502 A1

[22] www1.asminternational.org/asmenterprise/apd/AdvancedSearchAPD.aspx

[23] Ustinovshikov YI, Pushkarev BE, Sapegina IV. Inorg Mater 2006; 42(4): 354

[24] Lomova NV, Shabanova IN, Ustinovshikov YI. Inorg Mater 2008; 44(8): 818

[25] Guo S, Ng C, Lu J, et al. J Appl Phys 2011; 109: 103505

[26] Guo S, Ng C, Wang Z, et al. J Alloys Compd 2014; 583: 410

[27] Humphreys FJ, Hatherly M. Recrystallization and Related Phenomena. Oxford: Pergamon Press. 2004, p173, p337

[28] Komura S, Horita Z, Nemoto M, et al. J Mater Res 1999; 14(10): 4044

[29] Bauser M, Sauer G, Siegert, K. Extrusion. 2nd ed. ASM International. 2006, p170

[30] Furu T, Orsund R, Nes E. Acta Metall Mater 1995; 43(6): 2209

[31] Kotval PS, Nostor OH. TMS-AIME 1969; 245: 1275

[32] Gallagher PCJ. Metall Trans 1970; 1: 2429

[33] Seymour WE, Harker D. Trans AIME 1950; 188: 1001

[34] Avner SH. Introduction to Physical metallurgy. McGraw-Hill. 1964, p100

[35] Wolfenden A. Acta Metall 1971; 19: 1373

[36] Dunn CG. Acta Metall 1953; 1: 163

[37] Dunn CG. Acta Metall 1954; 2: 173

[38] Hillert M. Acta Metall1965; 13: 227

[39] Rajmohan N, Szpunar JA, Hayakawa Y. Acta Mater 1999; 47: 2999

[40] Gunther B, Kumpmann A, Kunze HD. Scripta Metall Mater 1992; 27: 833

[41] Simpson CJ, Aust KT, Winegard WC. Metall Trans 1971; 2: 987

[42] Gertsman VY, Birringer R. Scripta Metall Mater 1994; 30: 577

[43] Riontino G, Antonione C, Battezzati L. J Mater Sci 1979; 14: 86

[44] Fiedler HC. Metall Trans A 1977; 8: 1307

[45] Randle V, Horton D. Scripta Metal Mater 1994; 31(7): 891

[46] Lee SB, Hwang NM, Yoon DY. Metall Mater Trans A 2000; 31: 985

[47] Burke JE. TMS-AIME 1949; 180: 73

[48] Beck PA, Kremer JC, PemerLH.TMS-AIME 1948; 175: 372

[49] Beck PA, Towers J, Manly WD. TMS-AIME 1948; 175:162

[50] Burke JE, Turnbull D. Prog Metal Phys 1952; 3: 220

[51] Ralph B, Shim KB, Huda Z. Mater Sci Forum 1992; 94-96: 129-140

[52] Drolet JP, Galibois A. Acta Metall 1968; 16(12):1387

[53] Gavriljuk VG. High Nitrogen Steels: Structure, Properties, Manufacture, Applications. Springer. 1999, p155

[54] King HW. J Mater Sci 1966; 1: 79

[55] http://www.webelements.com/

Appendix 1.1

Table 1.1. Phases present in the various alloys investigated in the present study as inferred from available phase diagrams and determined by experimental analyses. Room temperature and high temperature are designated as rt and ht, respectively.

Alloy	Phase stability information obtained from phase diagrams	Homogenization temperature used in this study (°C)	Phases present after homogenization (experimentally determined)
FeNiCoCrMn	NA	1200	FCC (single-phase)
FeNiCoCr	NA	1200	FCC (single-phase)
FeNiCoMn	NA	1100	FCC (single-phase)
FeNiCrMn	NA	1100	Multi-phase
FeCoCrMn	NA	1100	Multi-phase
NICoCrMn	NA	1100	FCC (single-phase)
FeNiCo	600-800 °C: FCC; 500-600 °C: FCC+BCC	1200	FCC (single-phase)
FeNiCr	927-1400 °C: FCC; 300-927 °C: FCC+BCC	1200	FCC (single-phase)
FeNiMn	400 °C: MnNi rt; 25 °C: (Fe)rt + σ phase	1100	FCC (single-phase)
FeCoCr	1200-1400 °C: FCC+BCC; 1100 °C: FCC/FCC+BCC boundary; 700-1000 °C: FCC + σ phase	X	X
FeCoMn	600-1200 °C: FCC; 400 °C: FCC+BCC 300 °C: BCC+ β-Mn; 25 °C: FCC_1+FCC_2	1200	Multi-phase
FeCrMn	1200 °C: BCC; 750-1000 °C: σ phase; 700 °C: σ phase+$Cr_{0.25}Mn_{0.45}Fe_{0.30}$ 25 °C: BCC + σ phase	X	X
NiCoCr	927-1227 °C: FCC	1200	FCC (single-phase)
NiCoMn	25 °C: FCC	1100	FCC (single-phase)
NiCrMn	650-952 °C: FCC+BCC; 25 °C: FCC + σ phase	1050	Multi-phase
CoCrMn	25 °C: (Co) rt + σ phase + $CrMn_3$ rt	1100	Multi-phase
FeNi	360-1440 °C: FCC; 347-360 °C: FCC+$FeNi_3$ rt; 200-347 °C: (Fe)rt+$FeNi_3$ rt	1200	FCC (single-phase)

Table 1.1. Continued

Alloy	Phase stability information obtained from phase diagrams	Homogenization temperature used in this study (°C)	Phases present after homogenization (experimentally determined)
FeCo	985-1490 °C: FCC; 730-985 °C: BCC; below 730 °C: B2	X	X
FeCr	830-1600 °C: BCC; 700-830 °C: σ phase + BCC; 540-700 °C: σ phase; 0-540 °C: σ phase + BCC	X	X
FeMn	510-1310 °C: FCC; 250-510 °C: FCC + (Mn)rt; 0-250 °C: (Fe)rt + (Mn)rt	1200	Multi-phase
NiCo	0-1480 °C: FCC;	1200	FCC (single-phase)
NiCr	0-1346°C: FCC + BCC	X	X
NiMn	890-1040 °C: FCC; 760-890 °C: FCC + B2; 720-760 °C: $L1_0$+B2; 80-720 °C: $L1_0$	980	Multi-phase
CoCr	1282-1400 °C: FCC + BCC; 998-1282 °C: FCC + σ phase; 600-998 °C: (Co)rt + σ phase	X	X
CoMn	710-1180 °C: FCC; 545-710 °C: FCC + (βMn); 300-545 °C: MnCo rt	1100	Multi-phase
CrMn	890-1440 °C: BCC; 400-890 °C: BCC + Cr_2Mn_3 ht	X	X

NA—not available X—phase diagrams indicated BCC or multiple phases so experiments not performed

Table 1.2. Temperatures at which melting was observed to start in DSC measurements of the recrystallized FCC materials investigated in this study.

Alloy	Melting Temperature (°C)
FeNiCoCr	1422
FeNiCo	1451
FeNiCr	1391
NiCoCr	1417
FeNi	1430
NiCo	1462
Ni	1455

Table 1.3. Hall-Petch intercepts and slopes for the equiatomic alloys and pure Ni.

Alloy	Hall-Petch intercept, H_o (HV)	Hall-Petch slope k_H (HV·μm^{-2})
FeNiCoCr	118	165.5
FeNiCo	97.3	131.1
NiCoCr	146.5	197.3
FeNi	104.7	113.4
NiCo	62.2	167.1
Ni	68.6	34.3

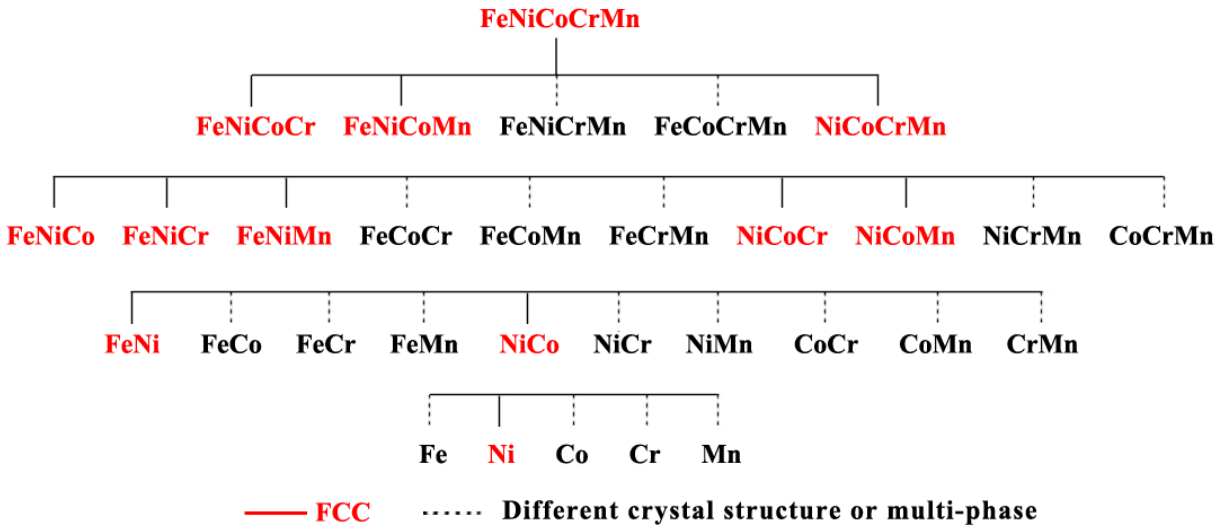

Fig. 1.1. All the possible quaternary, ternary, binary, and pure metal subsets of the quinary high-entropy alloy FeNiCoCrMn. After casting and homogenization, those that are single-phase FCC are identified in red, while those that are multi-phase or have a different crystal structure are identified in black.

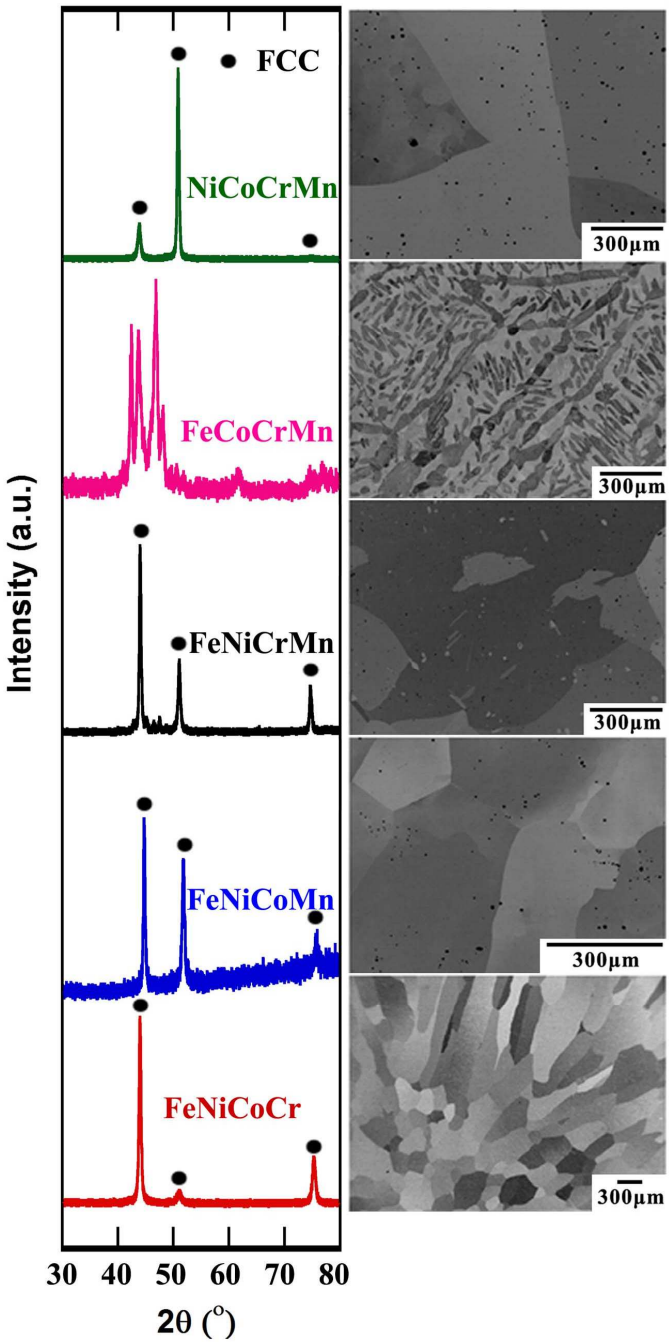

Fig. 1.2. XRD patterns and BSE images of the five quaternary equiatomic alloys investigated in this study in the cast and homogenized condition.

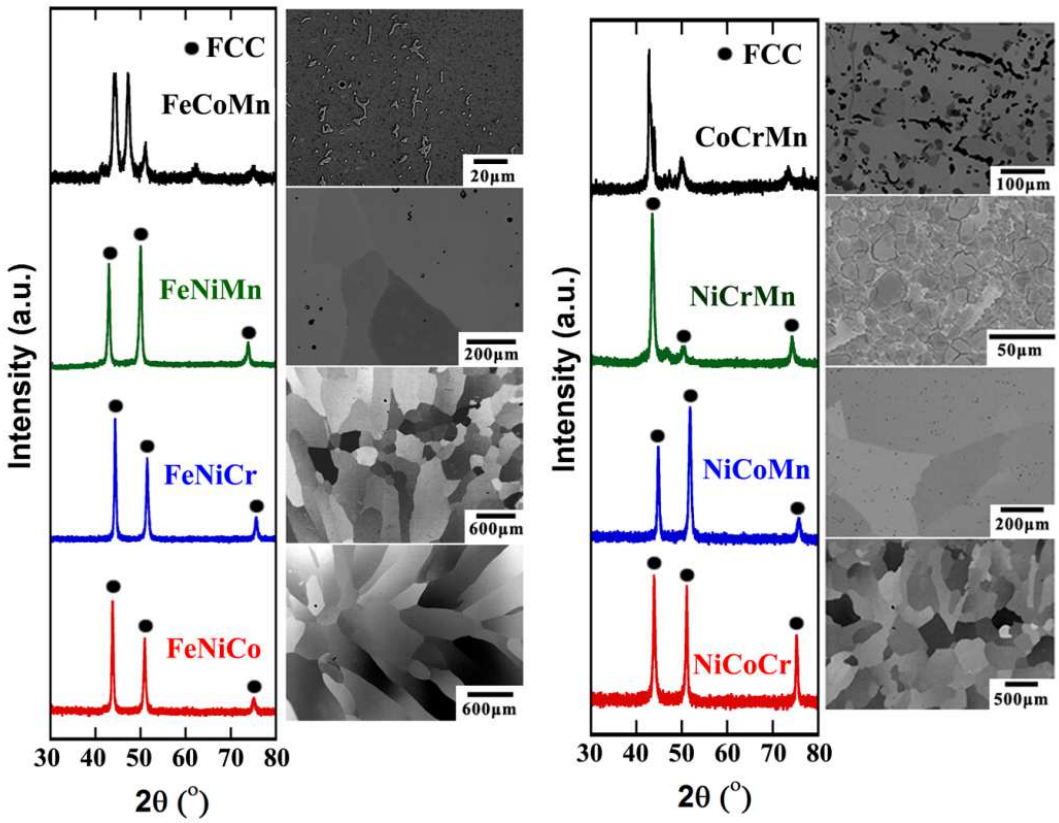

Fig. 1.3. XRD patterns and BSE images of the eight ternary equiatomic alloys investigated in this study in the cast and homogenized condition.

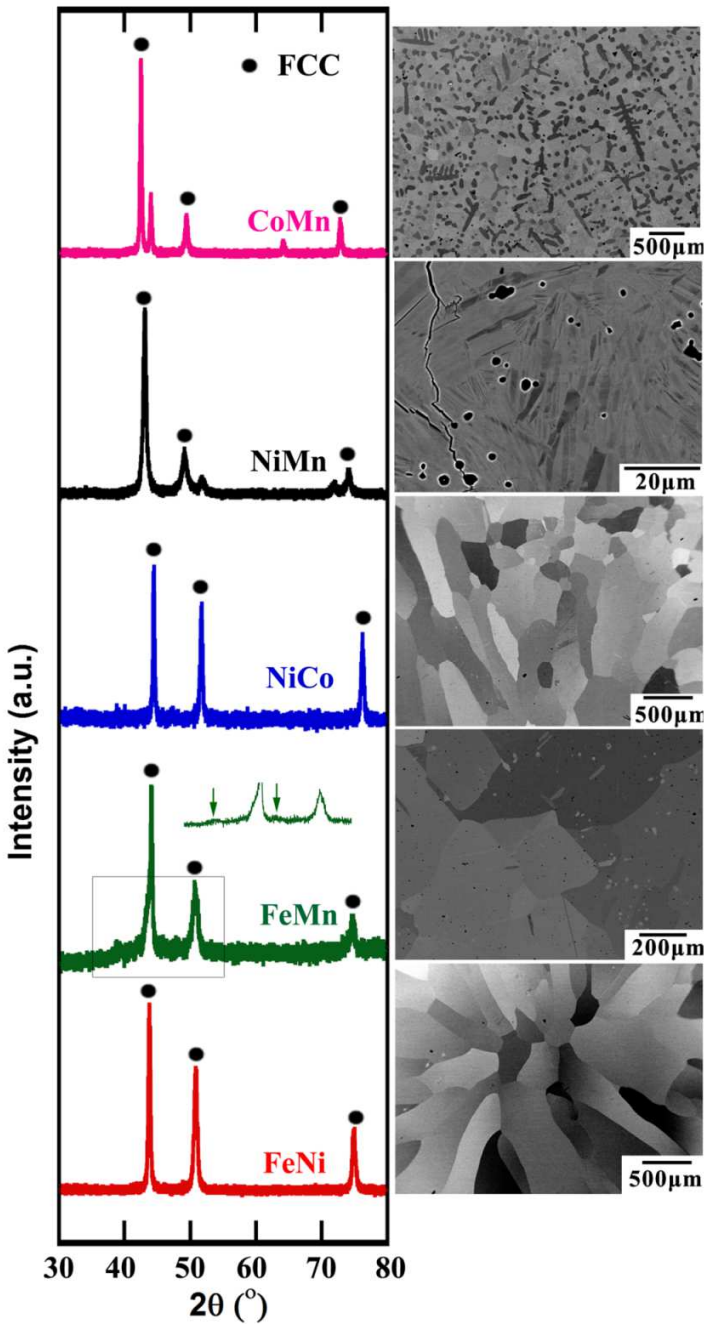

Fig. 1.4. XRD patterns and BSE images of the five binary equiatomic alloys investigated in this study in the cast and homogenized condition.

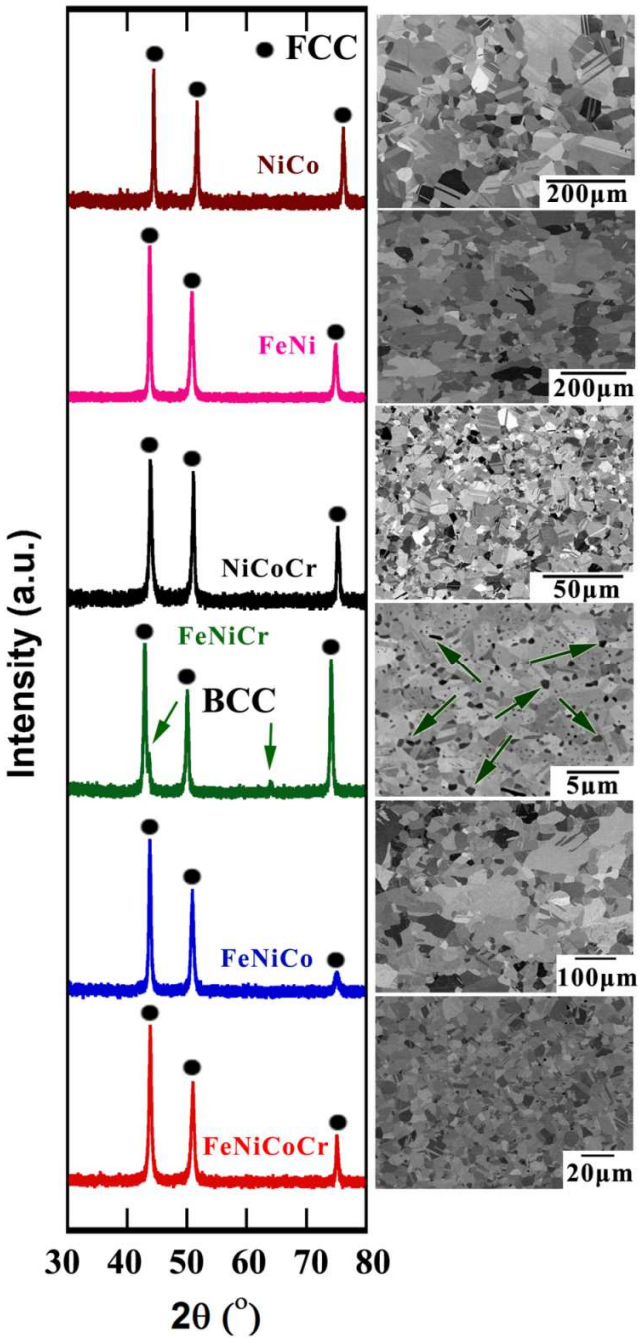

Fig. 1.5. XRD patterns and BSE images of the equiatomic alloys NiCo FeNi, NiCoCr, FeNiCr, FeNiCo, and FeNiCoCr after cold rolling and annealing at 800 °C for 1 hour. Green arrows in the XRD pattern and BSE image of FeNiCr indicate the BCC phase.

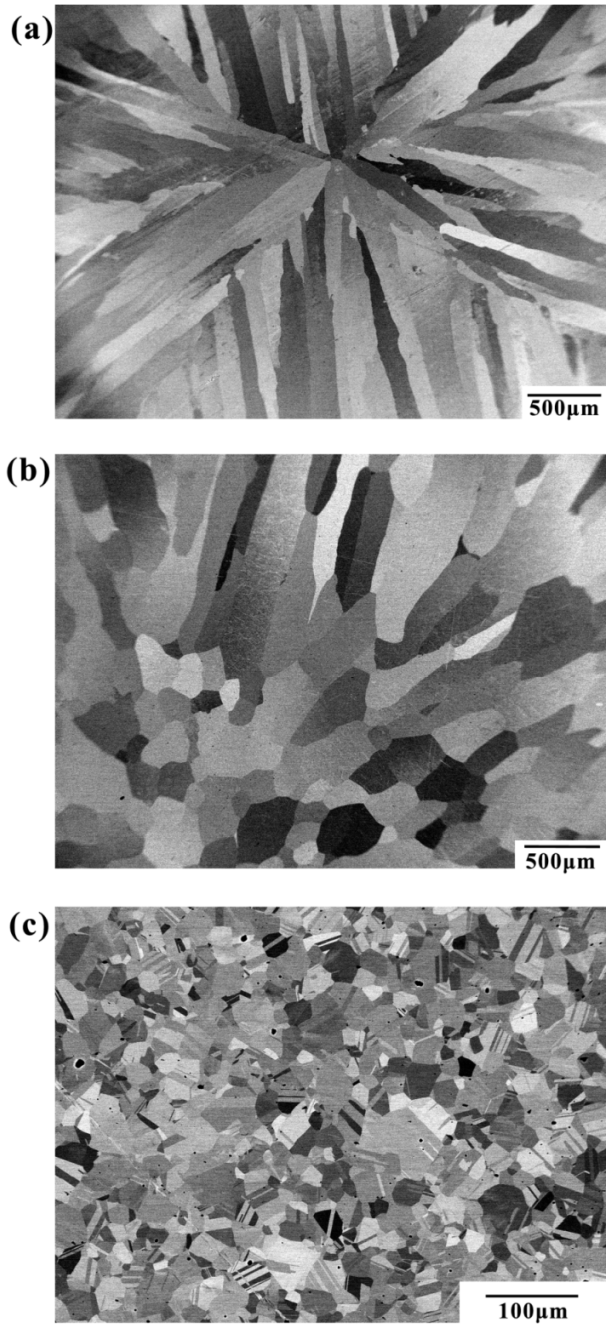

Fig. 1.6. Microstructures of the FeNiCoCr alloy: (a) in the as-cast state, (b) after homogenization at 1200 °C for 24 h and (c) after cold rolling and annealing at 900 °C for 1 h.

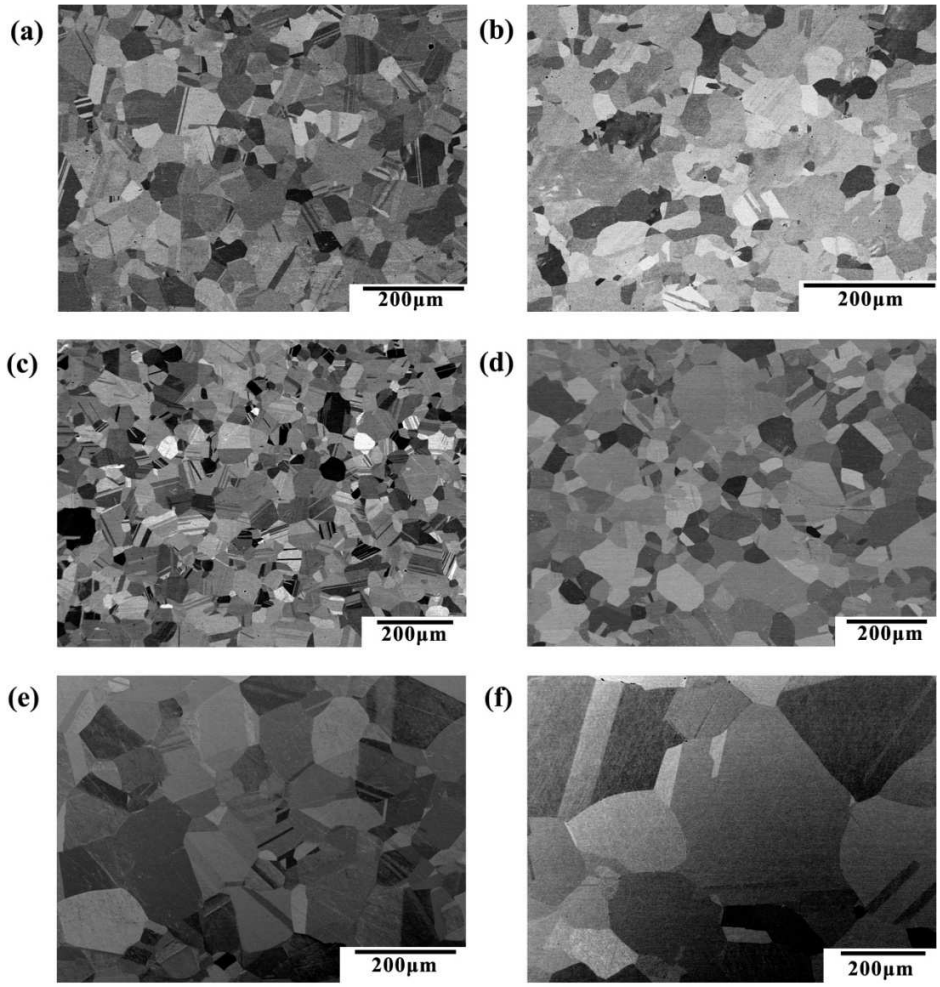

Fig.1.7. Microstructures of (a) FeNiCoCr, (b) FeNiCo, (c) NiCoCr, (d) FeNi, (e) NiCo and (f) Ni, after cold rolling and annealing at 1000 °C for 1 hour.

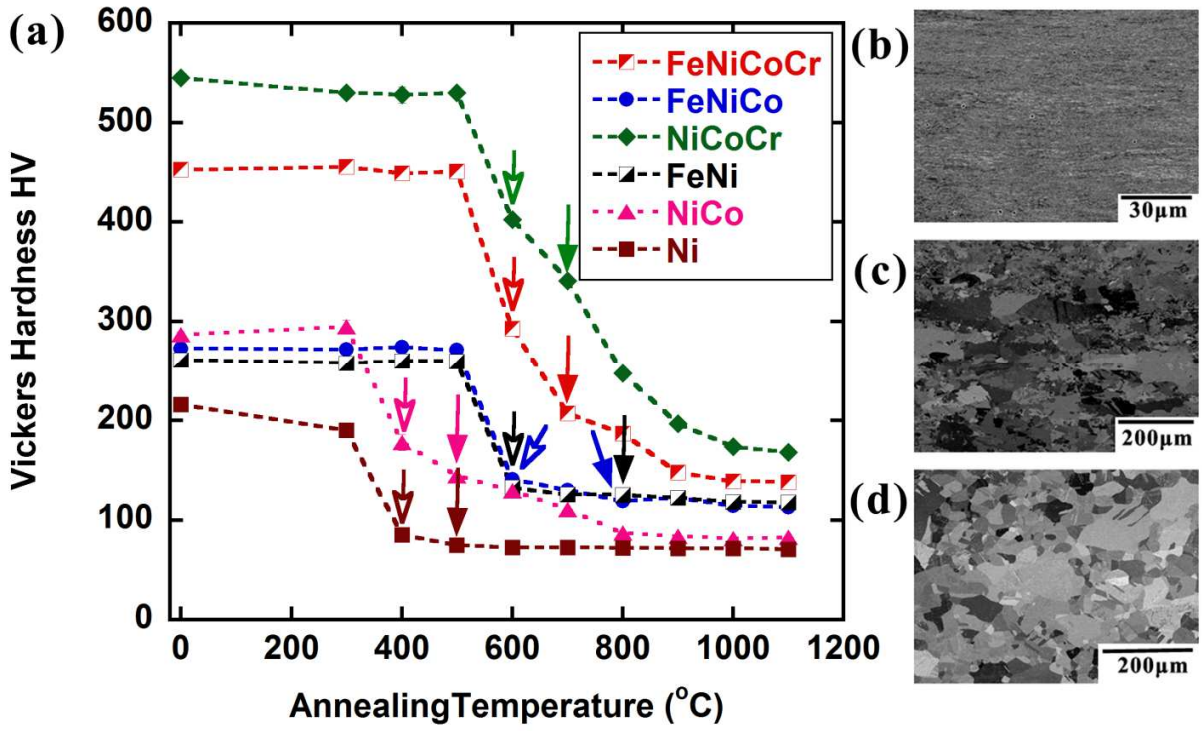

Fig. 1.8. (a) Microhardness of the equiatomic alloys and Ni after rolling and subsequent annealing at various temperatures for 1 h; the open and closed arrows represent approximately the start and finish of recrystallization, respectively. Representative examples of the microstructural evolution with annealing temperature are shown in the BSE images of the FeNiCo alloy annealed for 1 hour at (b) 500 °C, (c) 600 °C, and (d) 800 °C after cold rolling.

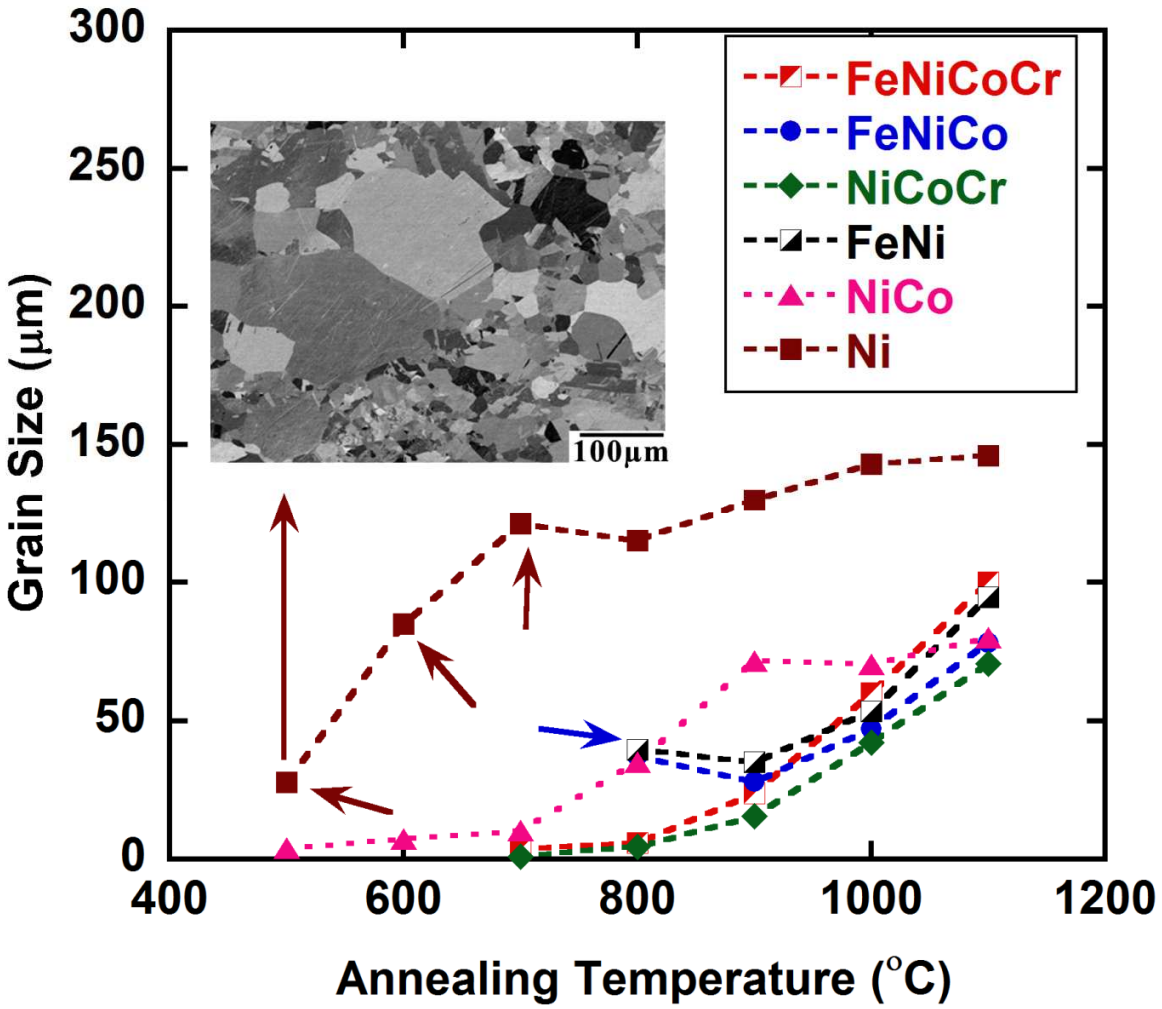

Fig. 1.9. Grain sizes of the recrystallized equiatomic alloys and pure Ni after annealing for 1 h at different temperatures. Inset shows an example of abnormal grain growthin pure Ni after 1-h anneal at 500 °C. The short arrows identify the four annealing temperatures at which abnormal grain growth was observed in FeNiCo and Ni.

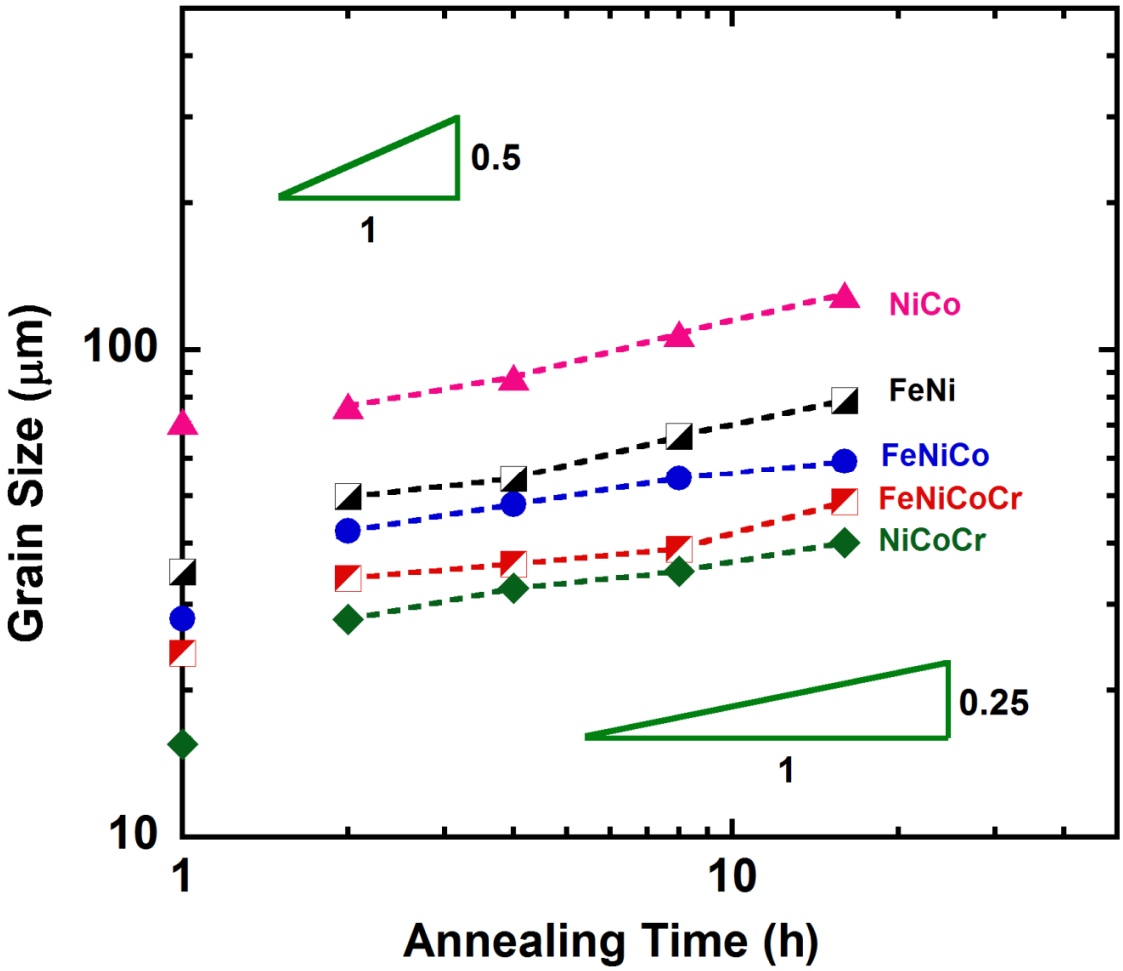

Fig. 1.10. Grain size as a function ofannealing time at 900 °C for the equiatomic alloys.

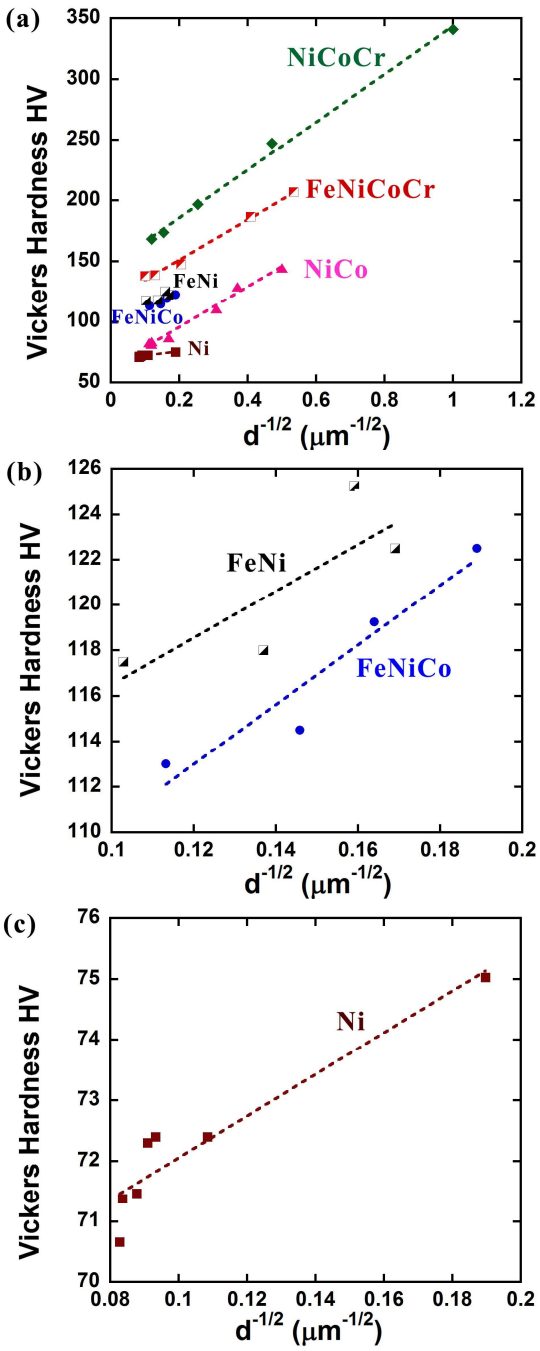

Fig. 1.11. (a) Microhardness as a function of grain size for the equiatomic alloys and pure Ni. Magnified views are shown in (b) for FeNi and FeNiCo, and (c) for Ni.

CHAPTER II

Temperature Dependence of the Mechanical Properties of Equiatomic Solid Solution Alloys with FCC Crystal Structures

A version of this chapter was submitted by Z. Wu, H. Bei, G.M. Pharr, E.P. George in 2014:

Z. Wu, H. Bei, G.M. Pharr, E.P. George. Temperature Dependence of the Mechanical Properties of Equiatomic Solid Solution Alloys with FCC Crystal Structures. Submitted to Acta Mater.

Authors:

Z. Wu

Materials Science and Engineering Department, University of Tennessee, Knoxville, TN 37996, USA

H. Bei

Materials Science and Technology Division, Oak Ridge National Laboratory, Oak Ridge, TN 37831, USA

G.M. Pharr, E.P. George

Materials Science and Engineering Department, University of Tennessee, Knoxville, TN 37996, USA; and Materials Science and Technology Division, Oak Ridge National Laboratory, Oak Ridge, TN 37831, USA

Z. Wu's involvement in the article: designed experimental procedures, prepared the samples, performed thermo-mechanical treatments and tensile tests, measured physical properties, analyzed the experimental data, wrote and revised the article.

Co-researchers' contributions are listed as follows:

H. Bei helped Zhenggang with the mechanical tests and physical property measurements, discussed the data and revised the article.

G.M. Pharr and E.P. George provided research guidelines and worked with Zhenggang to analyze the experimental data and revised the article.

Abstract

Compared to decades-old theories of strengthening in dilute solid solutions, the mechanical behavior of concentrated solid solutions is relatively poorly understood. A special subset of these materials includes alloys in which the constituent elements are present in equal atomic proportions, including the high-entropy alloys of recent interest. A unique characteristic of equiatomic alloys is the absence of “solvent” and “solute” atoms, resulting in a breakdown of the textbook picture of dislocations moving through a solvent lattice and encountering discrete solute obstacles. To clarify the mechanical behavior of this interesting new class of materials, we investigate here a family of equiatomic binary, ternary, and quaternary alloys based on the elements Fe, Ni, Co, Cr, and Mn that were previously shown to be single-phase face-centered cubic solid solutions.The alloys were arc-melted, drop-cast, homogenized, cold-rolled, and recrystallized to produce equiaxed microstructures with comparable grain sizes. Tensile tests were performed at an engineering strain rate of $10^{-3}\,s^{-1}$ at temperatures in the range 77-673 K. Unalloyed FCC Ni was processed similarly and tested for comparison. The flow stresses depend to varying degrees on temperature, with some (e.g., NiCoCr, NiCoCrMn and FeNiCoCr) exhibiting yield and ultimate strengths that increase strongly with decreasing temperature, while others (e.g., NiCo and Ni) exhibit very weak temperature dependencies. To better understand this behavior, the temperature dependencies ofthe yield strength and strain hardening were analyzed separately. Lattice friction appears to be the predominant component of the temperature-dependent yield stress, possibly because the Peierls barrier height decreases with increasing temperature due to a thermally induced increase of dislocation width. In the early stages of plastic flow (5~13% strain, depending on material), the temperature dependence of strain

hardening is due mainly to the temperature dependence of the shear modulus. In all the equiatomic alloys, ductility and strength increase with decreasing temperature down to 77 K.

1. Introduction

Dissolved solute atoms, to varying degrees, affect the mechanical properties of metals. Conventional treatments of solid solution strengthening assume that dislocations move through a solvent lattice of like atoms and encounter discrete unlike atoms (solutes) that can affect their mobility. The simplest case to consider is the energetics of, and the force resulting from, the elastic interaction of a dislocation with the strain field of a single solute atom [e.g., 1-7]. Both atomic size misfit and modulus mismatch between the solute and solvent atoms can contribute to this interaction. In reality, however, a dislocation interacts with multiple solute atoms simultaneously, and the net force exerted by all the solute atoms needs to be considered. For dilute solutions, early theories assumed that the interaction force between the dislocation and the solute atoms is either the maximum value possible (strong obstacles lying exactly in the slip plane), or zero (obstacles lying above or below the slip plane) [8, 9]. Taking into account the Friedel [10] separation between strong obstacles encountered by a dislocation, Fleischer developed a description in which the critical shear stress to overcome obstacles varied as the square root of the solute concentration, a result that was confirmedby early computer simulations [11, 12]. For more concentrated solutions, Labusch [13-15] developed a statistical treatment of a dislocation moving through an array of obstacles with a distribution of interaction strengths, rather than the binary interaction assumed in Fleischer's treatment, and obtained a critical shear stress that varied as the two-thirds power of solute concentration. Since the development of these early theories, there have been many refinements over the years [e.g., 16-21].

The picture of a dislocation moving through a solvent lattice and encountering discrete solute obstacles breaks down as the solute concentration and compositional complexity increase. Relatively little is known about the fundamental mechanisms of solid solution strengthening in

compositionally complex alloys, i.e., alloys comprised of multiple elements in high concentrations. An interesting subset of compositionally complex alloys is one in which the constituent elements are present in equal atomic concentrations. In such *equiatomic* alloys, there is no "solvent" or "solute" in the conventional sense. Therefore, rather than considering a dislocation moving through a solvent lattice and interacting with discrete solute atoms, it may be more appropriate to envisage the dislocation as moving through a mythical "average solvent" or "effective medium." In other words, the equiatomic alloy is not a simple extension or extrapolation from the dilute solution limits but rather a distinct new state akin to a stoichiometric compound with fixed atomic ratios, albeit disordered.

In order to develop accurate effective medium theories of solid solution strengthening, it is desirable to experimentally characterize the mechanical behavior of a range of equiatomic solid solution alloys. To this end, we investigate here several equiatomic binary, ternary and quaternary alloys that were previously shown to be single-phase face centered cubic (FCC) [22]. In addition, the alloys are all subsets of an equiatomic, quinary high-entropy alloy, FeNiCoCrMn, that is known to be a FCC-structured single-phase solid solution alloy [23-28]. Tensile tests showed that the yield and ultimate strengths of this high-entropy alloy increase as the temperature is decreased [24, 26].

The term high-entropy alloy (HE alloy) was coined by Yeh et al. [29] to denote alloys containing five or more elements in approximately equiatomic concentrations. These authors reasoned that the high configurational entropies of such alloys would stabilize the formation of a solid solution by counteracting the enthalpies of phase separation and compound formation. However, most of the so-called HE alloys discussed in the literature aremulti-phase alloys [e.g., 30-32] whose configurational entropies, as pointed out by Otto et al. [27], should in fact be low

rather than high. There are only a few multi-element alloys that are true single-phase solid solutions with FCC [23-28] or BCC crystal structures [33-35]. The configurational entropy of these single-phase alloys is likely to be high, approaching the value of the ideal mixture assumed in the analysis of Yeh et al. [29]. The present study of equiatomic binaries, ternaries, and quaternaries aims to provide an experimental basis to understand the mechanical behavior of all equiatomic alloys, including the more complex HE alloys containing five or more elements.

2. Experimental Methods

2.1. Alloy Preparation and Characterization

The equiatomic alloys listed in Table I were produced by arcmelting the elements Fe, Ni, Co, Cr, and Mn (>99.9% pure) in a water-cooled copper hearth under Ar atmosphere. All these alloys are single-phase, FCC solid solution alloys, as shown in an earlier paper [22], and all are subsets of the quinary, single-phase, FCC-structured, high-entropy alloy, FeNiCoCrMn [23-27]. For comparison, pure Ni was produced using the same process. When Mn was added as an alloying element, special care was taken in the processing because of its high vapor pressure and tendency to oxidize rapidly, as discussed elsewhere [22, 24, 26, 27]. The arc-melted buttons were flipped and re-melted at least five times to promote thorough mixing and then drop-cast into copper molds to produce rectangular ingots measuring 12.7 mm × 25.4 mm × 127 mm. The drop-cast ingots were homogenized for 24 hours at either 1373 or 1473 K (see Table 2.1), followed by water quenching. They were then cold rolled along the longitudinal ingot direction to a total thickness reduction of 90-92% (Table 2.1) without cross-rolling or intermediate annealing. Annealing studies were conducted on the rolled sheets to determine the temperatures and times

that would yield fully recrystallized microstructures and comparable grain sizes (see Table 2.1). In addition, the grain size of one of the alloys (FeNiCoCr) was systematically varied to investigate its influence on mechanical behavior.The annealed samples were ground (through 800-grit SiC paper), polished (through 20-nm colloidal silica suspension) and their microstructures examined in a JEOL 6500 SEM operated in the back-scattered electron (BSE) mode.

2.2. Tensile Tests

Flat dog-bone-type specimens with a gage length of 10 mm were cut from the cold-rolled sheets by electrical discharge machining (EDM) with their longitudinal axes perpendicular to the rolling direction. The specimens were annealed at the temperatures and times listed in Table 2.1, and all faces of their gage sections ground through 600-grit SiC paper. Nine Vickers microhardness indents spaced 1 mm apart were made along the specimen gage lengths using a LECO LM 100_{AT} Vickers Hardness tester witha force of 200 g. Uniform elongations to fracture were calculated by averaging the change in the distance between adjacent indents, excluding the two indents on either side of the fracture plane.

Tensile tests were performed with a screw-driven tensile testing machine (Instron) at an engineering strain rate of $10^{-3}\,s^{-1}$ and temperatures of 77, 203, 293, 473, and 673 K. For the tests below room temperature, the specimens and grips were first fully immersed in a bath of liquid nitrogen (77 K tests) or a dry ice plus ethanol mixture (203 K tests) for about 15 minutes before starting the test. During the tests, the baths were topped off as needed to keep the specimen and grips fully immersed at all times. Room-temperature tests were performed in ordinary ambient

air and those above room temperature in vacuum. X-ray diffraction was performed on the gage sections of specimens tested at 77 and 673 K to determine whether any phase transformation or second phase precipitation had occurred. No significant changes indicative of any phase transformations were observed on the XRD patterns. Fracture surfaces were examined in a JEOL JCM-5000 microscope operated at 10 kV.

2.3. Melting Temperature, Shear Modulus and Poisson's Ratio Measurements

The melting temperatures of the materials were measured using a NETZSCH 404 C differential scanning calorimeter (DSC). The melting point was determined during heating from room temperature as the start temperature of the endothermic melting peak observed on the DSC trace.

To determine the room-temperature elastic constants, densities were first measured with an AccuPyc 1330 pycnometer. Right cylindrical samples (7 mm length × 6 mm diameter) were cut from the homogenized ingots and ground through 600-grit SiC paper followed by compression to ~3 mm before being used for the density measurements. The purpose of this ~60% compression was to close up any casting pores that may have been present. After density measurements, the samples were annealed at 900 °C for 3 h to produce fully recrystallized microstructures. The annealed samples were carefully ground, their thicknesses measured, and time of flight measurements made with appropriate acoustic transducers to obtain longitudinal and shear wave velocities. Assuming the recrystallized (polycrystalline) materials are isotropic, their two independent elastic constants were calculated from the longitudinal and shear wave velocities using techniques described elsewhere [36].

The temperature dependence of the shear modulus of the FeNiCoCr alloy was measured using resonant ultrasound spectroscopy (RUS) using a commercial RUS system (RUSpec®, Quasar International Inc., Albuquerque, NM, USA) with a tripod transducer configuration. To make the measurements, a cylindrical ingot of this alloy, 25.4 mm in diameter, was cast and homogenized at 1473 K for 24 hours. A 7-mm-thick sliceof this ingot was then compressed to 3 mm and annealed at 1073 K for 3 hours. From this slice, a cylindrical specimen 25.4 mm in diameter and 3 mm thickwas cut using EDM and used for the RUS measurements. Additional details of the measurement procedures are described elsewhere [37].

3. Results and Discussion

Figure 2.1 shows the recrystallized microstructures of theequiatomic alloys and pure Ni after the annealing treatmentslistedin Table 2.1. The BSE images in this figure were taken on cross-sections perpendicular to the rolling direction. All of the alloys have equiaxed microstructures and similar grain sizes (24-48 μm), as summarized in Table 2.1, but with different densities of annealing twins. Unfortunately, a pure Ni specimen with a grain size in this range could not be produced. As discussed in a previous paper [22], Ni undergoes abnormal grain growthat temperatures below 1073 K when processed by the methods employed here. Normal grain growth occurs only at 1073 K and above. The smallest grain size we could produce at 1073 K was 85 μm, so the test results presented for pure Ni here are for this larger grain size.

Figure 2.2 shows the engineering stress vs. engineering plastic strain curves of the equiatomic alloys and pure Ni as a function of temperature.The curves were obtained from the tensile load-displacement data with the crosshead displacement calibrated using the elongation of the gage

length determined from the microhardness indents described earlier. To compute the plastic components of the strain, a line was fit to the linear elastic portion of the stress-strain curves and the amount of the elastic strain at a given point on the curve was subtracted from the total strain to obtain the plastic strain. In general, the flow stress (σ_{flow}) decreases with increasing temperature, and the stress-strain curves systematically shift up with decreasing temperature. Some of the alloys, namely, NiCoCr, FeNiMn, NiCoMn, FeNiCoMn and NiCoCrMn, exhibit pronounced serrations on their 673-K stress-strain curves that extend essentially from the yield point all the way to the startof necking. In two of the alloys, FeNiMn and NiCoMn, the serrations were also observed at 473 K. Such serrations are often associated with dynamic strain aging [38].

Figure 2.3 summarizes the 0.2% offset yield strengths (σ_y), ultimate tensile strengths (UTS), and uniform elongations to fracture, all of which increase with decreasing temperature, with maximum values attained at liquid nitrogen temperature (77 K). Since there are variations in the melting points of the different alloys (Table 2.2), we also plotted yield strengths versus homologous temperatures (not shown here). Basically the same trends and order of the different alloysas seen in Fig. 2.3 were observed also in the homologous temperature plots. At any given temperature, the alloys have large ranges of strength and ductility, with the ternary alloy, NiCoCr, havingthe highest valuesoverall.

Broadly speaking, there are two types of effectsevident in the mechanical properties shown in Figs. 2.2 and 2.3 – those due to the different alloying elements and thosedue to temperature. Considering first the former effect, it has been speculated [29] that equiatomic HE alloys will have higher strengths than conventional alloys containing just one principal element due to the higher degree of solid solution hardening from the increased number of elements. However, the current results show thatyield strength is not a simple function of the number of elements in the

equiatomic alloys. In fact, the yield strength does not increase monotonically as the number of elements increases: one of the ternary alloys (NiCoCr) has the highest strength, two of the quaternaries (FeNiCoCr and NiCoCrMn) are next, and all three have higher yield strengths (Fig. 2.3) than the five-element equiatomic alloy, FeNiCoCrMn [26]. Therefore, strength is not solely determined by the number of elements but also depends onthe type of added elements. In the present family of alloys, Cr appears to be the most potent strengthener. A similar behavior was observed previously inthe microhardness data of these alloys [22].

While traditional notions of solid solution hardening may shed some light on possible mechanisms by which composition affects strength, as noted before, because of their equiatomic compositions, there are no “solvents” or “solutes” in these alloys. Therefore, new “averaging” schemes may be needed to properly account for the complex atomic arrangements that are present both in the dislocation cores and in the surrounding lattice. Nevertheless, among the factors that can producesolid solution hardening, such as size misfit, modulus mismatch, stacking fault energy changes, and short-range ordering, the first two may be important based on trends observed in relatively dilute alloys [39]. For the elements in our alloys (Fe, Ni, Co, Cr and Mn), the largest (pair-wise) differences in atomic sizes and Young’s moduli are 3.7% between Ni and Mn [40] and 40.9% between Cr and Mn [41], respectively, suggesting that the observed differences in strength may be due to modulus mismatch rather than size misfit. However, further studies are needed to develop a deeper understanding of compositional effects in equiatomic alloys.

The second broad trend that can be seen in the data in Figs. 2.2 and 2.3 is that the flow stress, σ_{flow}, depends to varying degrees on the test temperature. It is convenient to think of the flow stress as consisting of two parts:(1) the yield stress (σ_y), which depends on the initial dislocation

density (ρ_i), and (2) an incremental hardening ($\Delta\sigma_\rho$) due to the evolution of dislocation density (ρ) with strain, such that:

$$\sigma_{flow}(T) = \sigma_y(T) + \Delta\sigma_\rho(T). \qquad (1)$$

Consequently, the temperature dependence of flow stress seen in Figs. 2.2 and 2.3 may be due to the temperature dependencies of either, or both, of the terms on the right hand side. In the following sections we address the potential mechanisms by which temperature can affect the yield strength and strain hardening behavior of the equiatomic alloys.

3.1. Effects of Temperature on Yield Strength

Because of their negligible Peierls-Nabarro barriers, the yield strengths of pure FCC metals are relatively insensitive to changes in temperature (at least at low homologous temperatures), as has been confirmed by previous studies [42-45], as well as our present results on pure Ni (Fig. 2.3a). Nevertheless, temperature-dependent yield strengths have been reported for binary FCC alloys, including Cu-Mn [46, 47], Cu-Al [48-50], Cu-Ge [51-53], Cu-Zn [54, 55], Cu-Ni [56], Au-Ag [56], and Al-Mg [57], with the yield strength typically increasing at lower temperatures. Both the thermal and athermal portions of the yield strength vs. temperature curves of these binaries often shift to higher values as the solute concentration increases [58, 59], suggesting an increase in the number of both short-range dislocation obstacles that can be overcome by thermal activation and longer range obstacles that cannot. Consistent with previous observations in binary alloys (most of which were relatively dilute solid solutions), the compositionally complex equiatomic alloys examined here also exhibit varying degrees of strengthening at lower

temperatures, with at least some, for example NiCoCr, NiCoCrMn, and FeNiCoCr, exhibiting significant strengthening as the temperature is decreased into the cryogenic range.

Yield stress is a combination of the frictional stress (σ_{fr}), or the intrinsic lattice resistance to dislocation motion, plus the various incremental strengthening contributions, such as those due to the initial dislocation density ($\Delta\sigma_{\rho i}$), solid solution hardening ($\Delta\sigma_{ss}$), precipitate hardening ($\Delta\sigma_{ppt}$), and grain boundary (Hall-Petch) strengthening ($\Delta\sigma_{gb}$). A general expression for the yield strength can therefore be written as:

$$\sigma_y = \sigma_{fr} + \Delta\sigma_{\rho i} + \Delta\sigma_{ss} + \Delta\sigma_{ppt} + \Delta\sigma_{gb} . \qquad (2)$$

In the present analysis, two of the terms on the right hand side ($\Delta\sigma_{ppt}$ and $\Delta\sigma_{\rho i}$) can be eliminated immediately. First, no precipitates are present in our alloys, at least based on their x-ray diffraction spectra and BSE images [22], both of which indicate that the alloys are single-phase solid solutions, so $\Delta\sigma_{ppt}$ can be ignored. Higher magnification transmission electron microscopy (TEM) also failed to reveal any precipitates in the related FCC quinary FeNiCoCrMn [26]. Since all the alloys investigated here are equiatomic FCC subsets of this "parent" alloy, it seems reasonable to assume that the lower order alloys are also free of second phases. Second, TEM of the equiatomic quinary alloy, FeNiCoCrMn, found that representative images from foils of the recrystallized alloy contained practically no dislocations [26]. Since the current alloys were processed similarly and fully recrystallized to produce comparable grain sizes, it is reasonable to assume that their initial dislocation densities are also very low. Assuming that is the case, we ignore the limited contribution of initial dislocation density to yield stressin our analysis.

Next, we address the third term on the right, $\Delta\sigma_{ss}$. Mechanistically, as mentioned before, solid solution strengthening has traditionally been considered in relatively dilute solutions where there is a solvent lattice through which the dislocations move and interact with discrete solute atoms. In such cases, the dislocation core is comprised almost exclusively of like (solvent) atoms that encounters unlike (solute) atoms as it moves through the lattice. At low solute concentrations, the flexibility of the dislocation line allows it to bend around obstacles and take on low-energy configurations. This becomes progressively more difficult as the spacing between obstacles decreases. In the limit of the equiatomic alloys, there is no "solvent" lattice through which the dislocations move and no "solute" atoms that they occasionally encounter, assuming the constituent atoms are truly randomly arranged on the FCC lattice. In this sense, the equiatomic alloys represent a new state of material more akin to a stoichiometric compound with fixed atomic ratios, albeit disordered, than a traditional dilute solid solution. When viewed in this light, it is logical to fold the solid solution hardening term ($\Delta\sigma_{ss}$) in Eq. (2) into the lattice friction term (σ_{fr}), where the latter now represents some "average" resistance offered by all the constituent atoms rather than a single type of solvent atom.This allows usto simplifythe expression for the yield strength to:

$$\sigma_y(T) = \sigma_{fr}(T) + \Delta\sigma_{gb}(T), \qquad (3)$$

where the temperature dependence of yield strength can be the result of either, or both, of the two terms on the right. In what follows, we first address the second term on the right, $\Delta\sigma_{gb}$, which is the contribution of grain boundaries to strength, and then focus mostly on the lattice friction σ_{fr}.

In the classical Hall-Petch treatment of grain boundary strengthening, a plot of yield strength versus the inverse square root of grain size is linear. Figure 2.4 issuch a plot for one of the quaternary equiatomic alloys, FeNiCoCr, at five different temperatures. If the grain boundary strengthening term in Eq. (3) were temperature-dependent, then the Hall-Petch slopes would vary with temperature. However, it is apparent that the slopes in Fig. 4 are all essentially the same. This, coupled with the fact that the alloys in Fig. 3a all had roughly the same grain size (Table 2.1), leads us to conclude that grain boundary strengthening does not contribute significantly to the observed temperature dependence of yield strength in the present study.

Therefore, the only remaining factor that could produce the observed temperature dependence of yield stress is a temperature-dependent lattice friction stress (σ_{fr}).To analyze this, we note that the Peierls-Nabarro stress (henceforth referred to as the Peierls stress, σ_p), which is commonly used to explain lattice friction, is given by[39]:

$$\sigma_p = \frac{2G}{1-\nu}\exp\left(\frac{-2\pi\omega}{b}\right), \qquad (4)$$

where G is the shear modulus, ν is Poisson's ratio, ω is the dislocation width, and b is the magnitude of the Burgers vector. The temperature dependencies of G and b in this expression can obviously lead to a small temperature dependence of the Peierls stress. However, it has been pointed out that the dislocation width ω can also be temperature dependent, and, since it appears in the expression inside the exponential, it may be the dominant factor. The dependence of dislocation width on temperature has been approximated by Dietze [60] as:

$$\frac{\omega}{b} = \left(\frac{\omega}{b}\right)_0 \exp\left(\frac{T}{3T_m}\right), \qquad (5)$$

where $\left(\frac{\omega}{b}\right)_0$ indicates values at 0 K, T is the test temperature, and T_m is the melting temperature. Ignoring the change of b with temperature, and using asimple Taylor expansion, we can rewrite equation (5) as:

$$\omega \approx \omega_0\left(1+\frac{T}{3T_m}\right), \qquad (6)$$

where ω_0 is the dislocation width at 0 K. This indicates a linear relationship between dislocation width and absolute temperature provided the temperature is low compared to the melting temperature, a relationship used previously by Petch [61]. Therefore, to a first approximation:

$$\omega = \omega_0(1+\alpha T), \qquad (7)$$

where α is a small positive constant. Combining equations (7) and (4), the temperature dependence of the Peierls stress becomes:

$$\sigma_p = \frac{2G}{1-\nu}\exp\left(\frac{-2\pi\omega_0}{b}\right)*\exp\left(\frac{-2\pi\omega_0}{b}\alpha T\right) \qquad (8).$$

From the above expression, the Peierls stress at 0 K can be obtained as:

$$\sigma_p(0) = \frac{2G}{1-\nu}\exp\left(\frac{-2\pi\omega_0}{b}\right) \qquad (9).$$

This suggests that if the temperature-dependence of yield stress is the same as that of the Peierls stress, the yield stress will decay with temperature in an exponential way.

To check the validity of these concepts, the yield stress data are re-plotted in Fig. 2.5, along with data obtained previously for the equiatomic quinary alloy FeNiCoCrMn of comparable

grain size [26]. It was found that the data are well described by curve fits (dashed lines) shown in Fig. 2.5 of the form:

$$\sigma_y(T) = \sigma_a \exp\left(\frac{-T}{C}\right) + \sigma_b, \qquad (10)$$

Where σ_a, C, and σ_b are fitting constants. When written this way, the first term on the right represents the thermal or temperature-dependent part of the yield strength and the second term is the temperature-independent or athermal part. Equating the temperature-dependent part of Eq. (10) with the temperature-dependent Peierls stress in Eq. (8) yields:

$$\sigma_a = \sigma_p(0) = \frac{2G}{1-\nu}\exp\left(\frac{-2\pi\omega_0}{b}\right) \qquad (11)$$

and

$$C = \frac{b}{2\pi\omega_0\alpha} \qquad (12).$$

Values of the parameters σ_a, C, and σ_b determined from least squares fits of the experimental data are listed in Table III. Since it has been shown [62, 63] that Eq. 4 is a reasonable approximation of the Peierls stress over the range ~0.4<ω/b< ~2.1 (i.e., 0.5b<ω < 2b), the table also includes values of the Peierls stressat 0 K, $\sigma_p(0)$, calculated from Eq. 9 assuming $\omega_0 = 0.5b$, b, 1.5b and 2b,which can be compared withthe values of σ_a found from the curve fits. The shear moduli and Poisson's ratiosused in the calculations were measured by ultrasonic techniques and are given in Table 2.2. For the equiatomic alloys, the calculated Peierls stress at 0 K ($\sigma_p(0)$) has the best match with the fitted σ_a values when $\omega_0 = b$. For pure Ni, on the other hand, the match is betterwhen $\omega_0 = 1.5b$. We are not aware of any published data for the dislocation widths in pure

Ni, but a value of 1.5*b* has been reported for pure Cu [53, 66], and this agrees well with the value derived here for Ni. The reasonable match between the calculated and fitted values lends credence to the analysis and suggests that the dislocations in the equiatomic alloys are narrower than in pure FCC metals. Additionally, the analysis suggests that the temperature dependence of the yield strength of the equiatomic alloys may be due to thermally-induced changes in dislocation width that, in turn, produce a temperature dependence of the Peierls stress.

To further check the validity of this analysis, values for α in Eq. (8) were calculated from the fitted *C* values by means of Eq. 12 where it was assumed that $\omega_0 = b$ for the equiatomic alloys and 1.5*b* for pure Ni. These are listed in Table 2.3, along with values for the product of α and T_m. For most of theequiatomic alloys and pure Ni, the product of α and T_m lies in the neighborhood of 1 (~0.8-1.5), implying that $\alpha \approx \frac{1}{T_m}$. Inserting this into equation (8) gives:

$$\sigma_p \approx \frac{2G}{1-\nu} \exp\left(\frac{-2\pi\omega_0}{b}\right) * \exp\left(\frac{-2\pi\omega_0}{bT_m}T\right) = \sigma_p(0) * \exp\left(\frac{-2\pi\omega_0}{bT_m}T\right) \qquad (13).$$

This expression is very similar to an equation derived by Dietze [60] to take into account the increase of dislocation width with temperature and consequent decrease in the Peierls stress:

$$\sigma_p \approx \sigma_p(0) * \exp\left(\frac{-2\pi\omega_0}{3bT_m}T\right) \qquad (14).$$

The only difference between equations (13) and (14) is the factor 3, which, as noted by Nabarro [65], isunlikely to be significant in light of the various assumptions made in the derivations.

It is generally believed that Peierls barriers are high in BCC metals and relatively low in FCC metals and that a major factor contributing to this difference is the relative widths of the

dislocations. The present analysis suggests that the dislocations in equiatomic FCC alloys may be narrower than those in pure FCC metals, which could lead to a stronger Peierls barrier and temperature dependence of strength. However, the temperature dependence of the equiatomic alloys, while stronger than that of pure FCC metals, is not as strong as that of BCC metals. Specifically, from room temperature to liquid nitrogen temperature the yield stress of the equiatomic FCC alloys increases by a factor of ~1.3-2.0 in comparison to a factor of ~3.5 for BCC metals such as iron [66] and tantalum [67]. Thus, the Peierls barrier height of the FCC equiatomic alloys is likely intermediate to that of pure FCC and BCC metals.

It should be noted that all of these arguments are premised on the notion that the primary source of the temperature dependence of the yield strength is the temperature-dependent height of the Peierls barrier. Other temperature dependences could accrue from the thermally activated processes that control dislocation mobility during glide, but these have not been explicitly addressed here. Detailed knowledge of the specific mechanisms responsible for these thermally activated processes would be needed to model them accurately in future investigations.

3.2. Effects of Temperature on Strain Hardening

Since flow stress depends on the yield stress and work hardening [Eq. (1)], either one or both could cause the observed temperature dependence of flow stress in the equiatomic alloys. As discussed above, yield stress does indeed depend on temperature, and its origin can be ascribed to a temperature-induced change in the dislocation width and friction stress. To investigate the temperature dependence of strain hardening, we first note that the engineering stress-strain curves of some of the equiatomic alloys in Fig. 2.2 appear to be parallel to each

other at different temperatures. If this is generally true, it implies that the strain-hardening component of the flow stress ($\Delta\sigma_\rho$) is essentially temperature independent, leaving the temperature dependence of the yield stress (σ_y) as the primary contributor. To determine whether this is in fact the case, the engineering stress-strain curvesin Fig. 2.2 were converted to true stress-strain curves and the 0.2% yield stress was subtracted from each value of stress to give the portion of the flow stress associated with strain hardening, $\Delta\sigma_\rho = \sigma_{flow} - \Delta\sigma_y$.The results are shown in Fig. 2.6. Clearly, the curves do not fully converge, indicating that the strain hardening ($\Delta\sigma_\rho$) does indeed depend on temperature to some extent.

The classical Taylor model [39] for strain hardening due to forest dislocations is usually described by

$$\Delta\sigma_p = \beta G b \rho^{\frac{1}{2}}, \qquad (15)$$

where β is a constant that depends on the strength of the dislocation-dislocation interaction, G is the shear modulus, b is the magnitude of the Burgers vector, and ρ is the dislocation density. Among the terms on the right hand side of Eq. 15, the shear modulus G is certainly temperature dependent. To investigate if this is the primary origin of the temperature dependence of the strain hardening, the isotropic shear modulus ofFeNiCoCr was measured at 293, 473 and 673 K using resonant ultrasound spectroscopy. The shear moduli of pure Ni at these temperatures were obtained from [68], and the modulus of FeNi was calculated from known single crystal elastic constants C_{11}, C_{12} and C_{44} [68] using the formula given by Hashin and Shtrikman [69]. Table 2.4 lists the measured and calculated shear moduli.

The strain hardening curves for FeNiCoCr, FeNi, and Ni in Fig. 2.6 were normalized using their respective temperature-dependent shear moduli in Table 2.4, and the resulting values ($\Delta\sigma_\rho/G$) are plottedin Fig. 2.7 as a function of plastic strain.These normalized curves generally converge up to certain strains, namely, ~13% for the two alloys and ~5% for pure Ni. This suggests that, at low strains, the temperature dependence of strain hardening in equation (14) is indeed mainly due to the temperature dependence of shear modulus and that dislocation multiplication, interaction and accumulation occur in a temperature-independent manner during the early stages of plastic deformation.

In addition to displaying higher strengths, many of the equiatomic alloys are significantly more ductile than pure Ni, and their ductilities generally increase with decreasing temperature, as shown in Fig. 2.3. Similar trends were reported in earlier papers on high and medium entropy alloys [24, 26], where the high ductilities were ascribed to their high work hardening capability, which postpones the onset of necking instability according to Considere's criterion. To evaluate whether its role in the present study, the extent of work hardening, defined here as the difference between the ultimate tensile strength (UTS) and the yield strength, is plotted as a function of temperature in Fig. 2.8 for the equiatomic alloys and pure Ni. To varying degrees, the work hardening capability of all the materials increases with decreasing temperature, similar to what was observed before in the equiatomicquinary alloy FeNiCoCrMn [24, 26], as well as in other FCC alloys [70-75]. It appears therefore that this may be the reason for the increasing ductility with decreasing temperature.

One of the mechanisms for the much higher work hardening capability at cryogenic temperatures in the FeNiCoCrMn alloy is deformation-induced twinning [26], which can provide strengthening because of the additional internal twin boundaries generated, the so-called

"dynamic Hall-Petch" effect. Deformation twinning occurs in FCC metals and alloys with low stacking fault energy (γ_{SFE}) such as 70:30 brass, [76], but not in FCC metals with medium or high stacking fault energy such as Al [77]. The critical stacking fault energy below which twinning occurs in FCC materials has been reported to be ~45 mJ/m^2. At higher stacking fault energies (>45mJ/m^2), deformation is controlled by dislocation glidewhereasatvery lowstacking fault energies (<18 mJ/m^2), martensitic transformation is favored over deformation twinning [78, 79]. At low temperatures, even materials with γ_{SFE}> 45mJ/m^2 are found to be mechanically twinned, for example, Cu [80], whose γ_{SFE} is ~80 mJ/m^2 [39]. Even in pure Ni (γ_{SFE} ~ 150 mJ/m^2) [39], deformation twinning occurs under shock loading conditions [81]. Previous studies have shown that the addition of Fe, Co, Cr and Mn to pure Ni all reduce thestacking fault energy, with Cr having the largest effect and Fe the smallest [82, 83]. Additional work is needed to confirm whether, and to what extent, twinning contributes to work hardening in the present alloys. Martensitic transformation appears not to be a contributing factor since post-fracture x-ray diffraction performed on specimens tested at 77 K revealed no new phases.

The representative fracture surfaces in Fig. 2.9 show that there is significantly less macroscopic necking in the equiatomic alloy, FeNi, than in pure Ni, consistent with its higher tensile ductility and work hardening capability that postpones the onset of necking instability according to Considere's criterion. Microscopically, however, both exhibit ductile dimpleson theirfracture surfaces.A similar lack of necking was observed in the other equiatomic alloys that exhibited high ductilities. Microscopically, all the FCC alloys examined here exhibited ductile dimples on their fracture surfaces.

5. Summary and Conclusions

Several binary, ternary and quaternary alloys with equiatomic compositions were arc-melted, cast, cold rolled and recrystallized to produce equiaxed grains of comparable size. All the alloys are subsets of a quinary FCC high-entropy alloy that was previously investigated (FeNiCoCrMn) and consisted of single-phase solid solutions with the FCC structure. For comparison, unalloyed FCC Ni was also investigated. The effects of temperature on tensile properties were quantified over the temperature range of 77-673 K yielding the following observations:

(1) The flow stress of the equiatomic alloys is temperature dependent to varying degrees depending on the alloy. The yield and ultimate strengths of NiCoCr, NiCoCrMn, and FeNiCoCr increase strongly with decreasing temperature whereas those of NiCo and Ni exhibit very weak temperature dependencies.

(2) Alloying affects both the thermal and athermal portions of the yield stress vs. temperature curves.

(3) The stronger alloys are not necessarily the ones with the most elements. The nature of the constituent elements is also important, with the Cr-containing alloys in general being the strongest.

(4) The Hall-Petch slopes of the FeNiCoCr alloy are essentially independent of test temperature. This implies that grain-boundary strengthening is unlikely to be a major contributor to the observed temperature dependence of the yield strength.

(5) An analysis suggests that the temperature dependence of the yield strength in the alloys may be determined by Peierls-barrier-dominated lattice friction, with the height of the Peierls barrier controlled by thermal influences on the width of the dislocation. By fitting the experimental yield stress vs. temperature curves to the Peierls-Nabarro equation, the

barriers in the equiatomic FCC alloys appear to be stronger than those in pure FCC metals but weaker than those in pure BCC metals.

(6) The ultimate tensile strength and uniform elongation to fracture of all the equiatomic alloys increase with decreasing temperature, with the largest increase occurring between 77 and 293 K. It is possible that deformation twinning similar to that observed in the FeNiCoCrMn high-entropy alloy [26] contributes to the enhanced ductility atcryogenic temperatures in some of the alloys. Additional work is needed to verify this.

(7) During the initial stages of plastic deformation (5-13% strain, depending on material), the temperature dependence of strain hardening is due almost entirelyto the temperature dependence of the shear modulus. This indicates the athermal nature of dislocation multiplication, accumulation and interaction during the early stages of deformation.

Acknowledgments: This research was supported by the U.S. Department of Energy, Office of Basic Energy Sciences, Materials Sciences and Engineering Division. The authors thank Dr. Fei Renfor measuring the temperature dependence of the shear modulus of the quaternary alloy FeNiCoCr (Table 2.4).

References

[1] Cottrell AH. Dislocations and Plastic Flow in Crystals. Oxford University Press 1953.

[2] Eshelby JD. Acta Metall 1955; 3: 487.

[3] Cochardt AW, Schoeck G, Wiedersich H. Acta Metall 1955; 3: 533.

[4] Schoeck G, Seeger A. Acta Metall 1959; 7: 469.

[5] Mott NF, Nabarro FRN. Proc Phys Soc 1940; 52: 86.

[6] Cottrell AH, Bilby BA. ProcPhysSoc A 1949; 62: 49.

[7] Dijkstra LJ. J Met 1949; 1: 252.

[8] Fleischer RL. Acta Metall 1961; 9: 996.

[9] Fleischer RL. Acta Metall 1963; 11: 203.

[10] Friedel J. Dislocations. Pergamon Press 1964.

[11] Foreman AJE, Makin MJ. Philos Mag 1966; 13: 13.

[12] Kocks UF. Philos Mag 1966; 13: 541.

[13] Labusch R. Phys Stat Sol 1970; 41: 659.

[14] Labusch R. Acta Metall 1972; 20: 917.

[15] Labusch R. J Appl Phys 1977; 48: 4550.

[16]Arsenault RJ, Patu S, Esterling DM. Metall Trans A 1989; 20: 1411.

[17] Arsenault RJ, Patu S, Esterling DM. Metall Trans A 1989; 20: 1419.

[18] Leyson GPM, Hector LG, Curtin WA. Acta Mater 2012; 60: 3873.

[19] Leyson GPM, Curtin WA. Philos Mag 2013; 93: 2428.

[20] Leyson GPM, Curtin WA, Hector LG, et al. Nature Materials 2010; 9: 750.

[21] Roth HA, Davis CL, Thomson RC. Metall Mater Trans A 1997; 28: 1329.

[22] Wu Z, Bei H, Otto F, et al. Intermetallics 2014; 46:131.

[23] Cantor B, Chang ITH, Knight P, et al. Mater Sci Eng A 2004; 375-377: 213.

[24] Gali A, George EP. Intermetallics 2013; 39:74.

[25] Liu WH, Wu Y, He JY, et al. Scripta Mater 2013; 68: 526.

[26] Otto F, Dlouhy A, Somsen Ch, et al. Acta Mater 2013; 61: 5743.

[27] Otto F, Yang Y, Bei H, et al. Acta Mater 2013; 61(7): 2628.

[28] Zhu C, Lu ZP, Nieh TG. Acta Mater 2013; 61(8): 2993.

[29] Yeh JW, Chen SK, Lin SJ, et al. Adv Eng Mater 2004; 6: 299.

[30] Tang Z, Gao MC, Diao H, et al. JOM 2013; 65(12): 1848.

[31] Guo S, Ng C, Liu CT. J Alloys Compd 2013; 557: 77.

[32] Wang Z, Guo S, Liu CT. JOM 2014; DOI: 10.1007/S11837-014-0953-8.

[33] Senkov ON, Scott JM, Senkova SV, et al. J Alloys Compd 2011; 509: 6043.

[34] Senkov ON, Wilks GB, Miracle DB, et al. Intermetallics 2010; 18: 1758.

[35] Senkov ON, Wilks GB, Scott JM, et al. Intermetallics 2011; 19: 698.

[36] Bei H, George EP, Pharr GM. Scripta Mater 2004; 51: 875.

[37] RenF, Case ED, Ni JE, etal.Philos Mag2009; 89(2): 143.

[38] Robinson JM, Shaw MP. Int Mater Rev 1994; 39: 113.

[39] Dieter GE. Mechanical Metallurgy. McGraw-Hill Higher Education 1986.

[40] King HW.J Mater Sci 1966; 1: 79.

[41] http://www.webelements.com/

[42] Low JR. Behavior of Metals at Low Temperatures. ASM 1952.

[43] Tetelman AS, McEvily AJ. Fracture of Structural Materials. John Wiley & Sons, Inc 1966.

[44] Liu A. Mechanics and Mechanisms of Fracture. ASM International 2005.

[45] Garstone J, Honeycombe RWK. Dislocations and Mechanical Properties of Crystals. John-Wiley 1957.

[46] Butt MZ, Rafi Z, Khan MA. Phys Stat Sol (a) 1990; 120: K149.

[47] Schwink CH, Wille TH. Scripta Metall 1980; 14: 1093.

[48] Demirskiy VV, Komnik SN, Starstsev VI. Phys Met Metall 1979; 46:151.

[49] Suzuki H. in: McQueen HJ, Bailon JP, Dickson JJ, et al. Strength of Metals and Alloys, Pergamon Press, 1985, 3: 1727.

[50] Koppenaal TJ, Fine ME. Trans AIME 1962; 224: 347.

[51]Kamada K, Yoshizawa IJ. Phys Soc Jpn 1971; 31(4): 1056.

[52] Traub H, Neuhauser H, Schwink CH.ActaMetall 1977; 25: 437.

[53] Feltham P, Copley GJ. Acta Metall 1960; 8: 542.

[54] Butt MZ, Ghauri IM. Phys Stat Sol (a) 1988; 107: 187.

[55] Ardley GW, Cottrell AH. Proc R Soc Lond 1953; 219: 328.

[56] Suzuki H. in: Kettunen PO, Lepisto TK, Lehtonen ME. Strength of Metals and Alloys (ICSMA 8), Vol. 2, Pergamon Press, Oxford, 1988, 573.

[57] Butt MZ. J Mater Sci Lett 1988; 7: 879.

[58] Mitchell TE. in: Standford EG, Fearon JH. McGonnagle WJ. Progress in Applied Materials Research 1964; 6: 117

[59] Honeycombe RWK. The Plastic Deformation of Metals. ASM 1975.

[60] Dietze HD. Z Phys 1952; 132: 107.

[61] Petch NJ. Philos Mag A 1958; 3: 1089.

[62] Nabarro FRN. Philos Mag A 1997; 75(3): 703.

[63] Ohsawa K, Koizumi H, Kirchner OK,et al. Philos Mag A 1994; 69: 171.

[64] Seeger A, Schoeck G. ActaMetall 1953; 1: 520.

[65] Nabarro FRN. Mater Sci Eng A 1989; 113: 315.

[66] Hutchison MM. Philos Mag A 1963; 8: 121.

[67] Bethtold JH. ActaMetall 1955; 3: 249.

[68] Ledbetter HM, Reed RP. J Phys Chem Ref Data 1973; 2(3): 53.1.

[69] Hashin Z, Shtrikman S. J MechPhys Solids 1962; 10: 343.

[70] Rémy L, Pineau A. Mater SciEng 1976; 26: 123.

[71] Rémy L. ActaMetall 1978; 26: 443.

[72] Asgari S, El-Danaf E, Kalidindi R, Doherty R. Metall Mater Trans A 1997; 28: 1781.

[73] Rohatgi A, Vecchio KS, Gray GT. Metall Mater Trans A 2001; 32: 135.

[74] Beladi H, Timokhina IB, Estrin Y, Kim J, De Cooman BC, Kim SK. Acta Mater 2011; 59: 7787.

[75] Gutierrez-Urrutia I, Raabe D. Acta Mater 2011; 59: 6449.

[76] Hatherly M. in: Gifkins RC. Strength of Metals and Alloys (ICSMA 6), Vol. 3, Pergamon Press, Oxford, 1982, 1181.

[77] Huang CX, Wang K, Wu SD, et.al. Acta Mater 2006; 54: 655.

[78] Curtze S, Kuokkala VT. Acta Mater 2010; 58: 5129.

[79] Frommeyer G, Brüx U, Neumann P. ISIJ International 2003; 43: 438.

[80] Weiner D. Acta Metall 1972; 20: 1235.

[81] Nolder RL, Thomas G. Acta Mater 1963; 11: 994.

[82] Kotval PS, Nostor OH. TMS-AIME 1969; 245: 1275.

[83] Gallagher PCJ. Metall Trans 1970; 1: 2429.

Appendix 2.1

Table 2.1. Processing conditions and grain sizes of the equiatomic alloys.

Alloy	Homogenization temperature (K)	Reduction in thickness (%)	Annealing temperature (K), time (h)	Grain size (μm)
FeNiCoCr	1473	92	1173, 1	24
FeNiCoMn	1373	90	1273, 1	48
NiCoCrMn	1373	90	1273, 1	36
FeNiCo	1473	92	1173, 1	28
NiCoCr	1473	92	1273, 1	41
FeNiMn	1373	90	1173, 1	30
NiCoMn	1373	90	1173, 1	32
FeNi	1473	92	1173, 1	35
NiCo	1473	92	1073, 1	35
Ni	1473	92	1073, 0.5	85

Table 2.2. Measured melting temperatures, room temperature shear moduli and Poisson's ratios of the equiatomic alloys.

Alloy	Melting temperature (K)	Shear modulus (GPa)	Poisson's ratio
FeNiCoCrMn	1553	80	0.26
FeNiCoCr	1695	84	0.28
FeNiCoMn	1533	77	0.22
NiCoCrMn	1489	78	0.25
FeNiCo	1724	60	0.35
NiCoCr	1690	87	0.30
FeNiMn	1473	73	0.24
NiCoMn	1462	77	0.23
FeNi	1703	62	0.34
NiCo	1735	84	0.29
Ni	1728	76	0.31

Table 2.3. The fitting parameters σ_a, C, and σ_b obtained from curve fits of the data in Fig. 5 according to the form of Eq. 10. The table also lists: the 0 K Peierls stress, $\sigma_p(0)$, calculated by assuming ω_0 = 0.5b, b, 1.5b, and 2b; the constant α; the melting temperatures (T_m); and the product of α and T_m. Additional descriptions of the parameters and their symbols are given in the text.

alloy	σ_a (MPa)	C (K)	σ_b (MPa)	$\sigma_p(0)$ (MPa) (ω_0=0.5b)	$\sigma_p(0)$ (MPa) (ω_0=b)	$\sigma_p(0)$ (MPa) (ω_0=1.5b)	$\sigma_p(0)$ (MPa) (ω_0=2b)	α (K^{-1})	T_m(K)	T_m*α
FeNiCoCrMn	423	180	109	9358	405	17	0.76	0.00088	1553	1.37
FeNiCoCr	443	184	184	9858	426	18	0.80	0.00087	1695	1.46
FeNiCoMn	282	219	101	8545	369	16	0.69	0.00073	1533	1.11
NiCoCrMn	491	207	166	9002	389	16	0.73	0.00077	1489	1.14
FeNiCo	292	252	125	7990	345	14	0.65	0.00063	1724	1.08
NiCoCr	489	228	167	10758	465	20	0.87	0.00070	1690	1.18
FeNiMn	283	195	182	8314	359	15	0.67	0.00082	1473	1.20
NiCoMn	302	190	170	8656	374	16	0.70	0.00084	1462	1.22
FeNi	341	291	74	8000	346	14	0.65	0.00055	1703	0.93
NiCo	130	336	50	10241	443	19	0.83	0.00047	1735	0.82
Ni	46	308	70	9534	412	17	0.77	0.00052	1728	0.89

Table 2.4. Temperature dependence of the shear modulus of FeNiCoCr (this study), FeNi (calculated from [68]), and pure Ni (extractedfrom [68]).

	Shear modulus (GPa)		
Temperature (K)	FeNiCoCr	FeNi	Ni
77	--	68	84
203	--	66	80
293	84	62	76
473	79	62	73
673	72	60	70

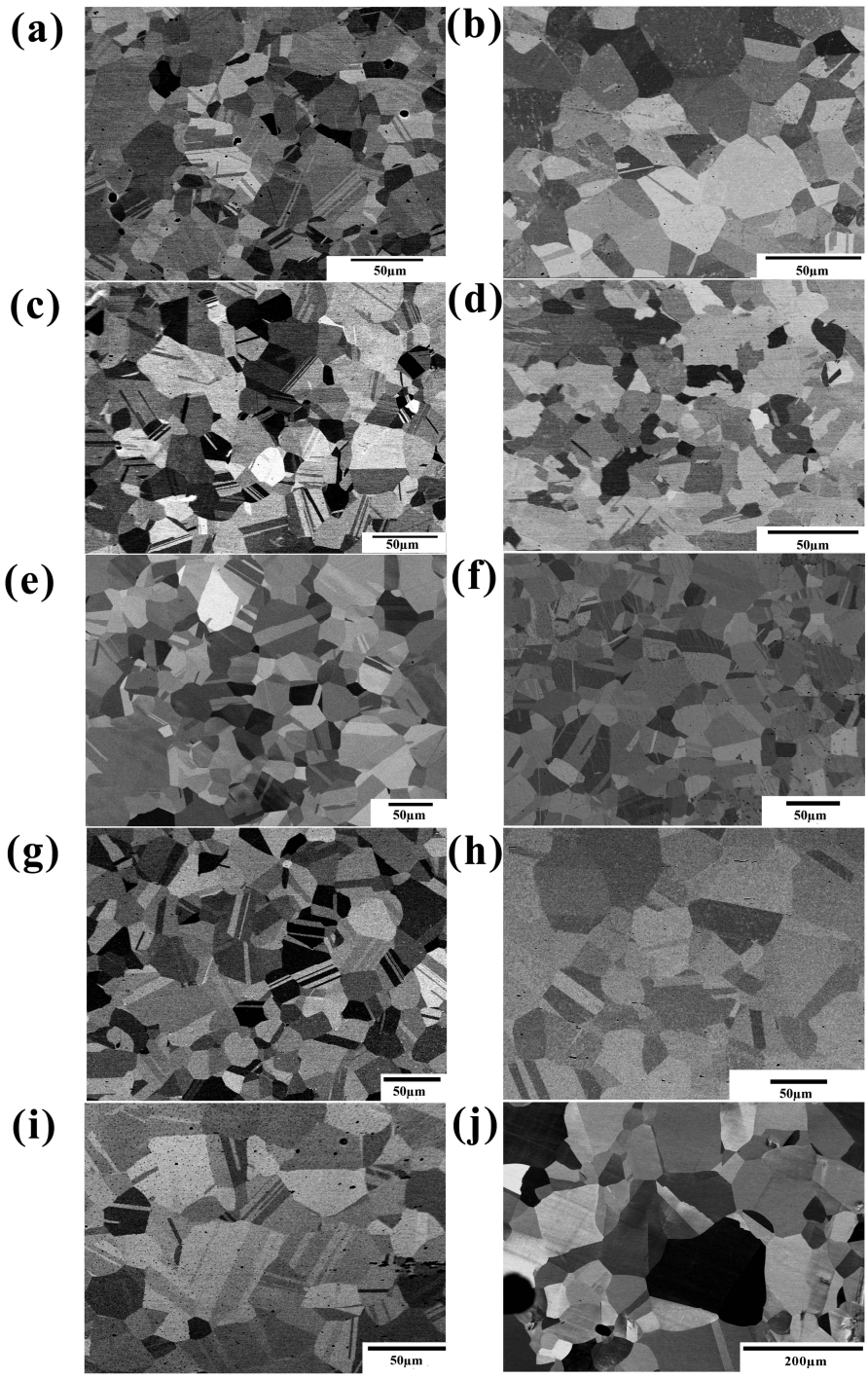

Fig. 2.1. Back-scattered electron images of: (a) FeNiCoCr, (b) FeNiCo, (c) NiCoCr, (d) FeNi, (e) NiCo, (f) FeNiMn, (g) NiCoMn, (h) FeNiCoMn, (i) NiCoCrMn,and (j) pure Ni after cold-rolling and annealing (annealing temperatures and times are shown in Table 2.1).

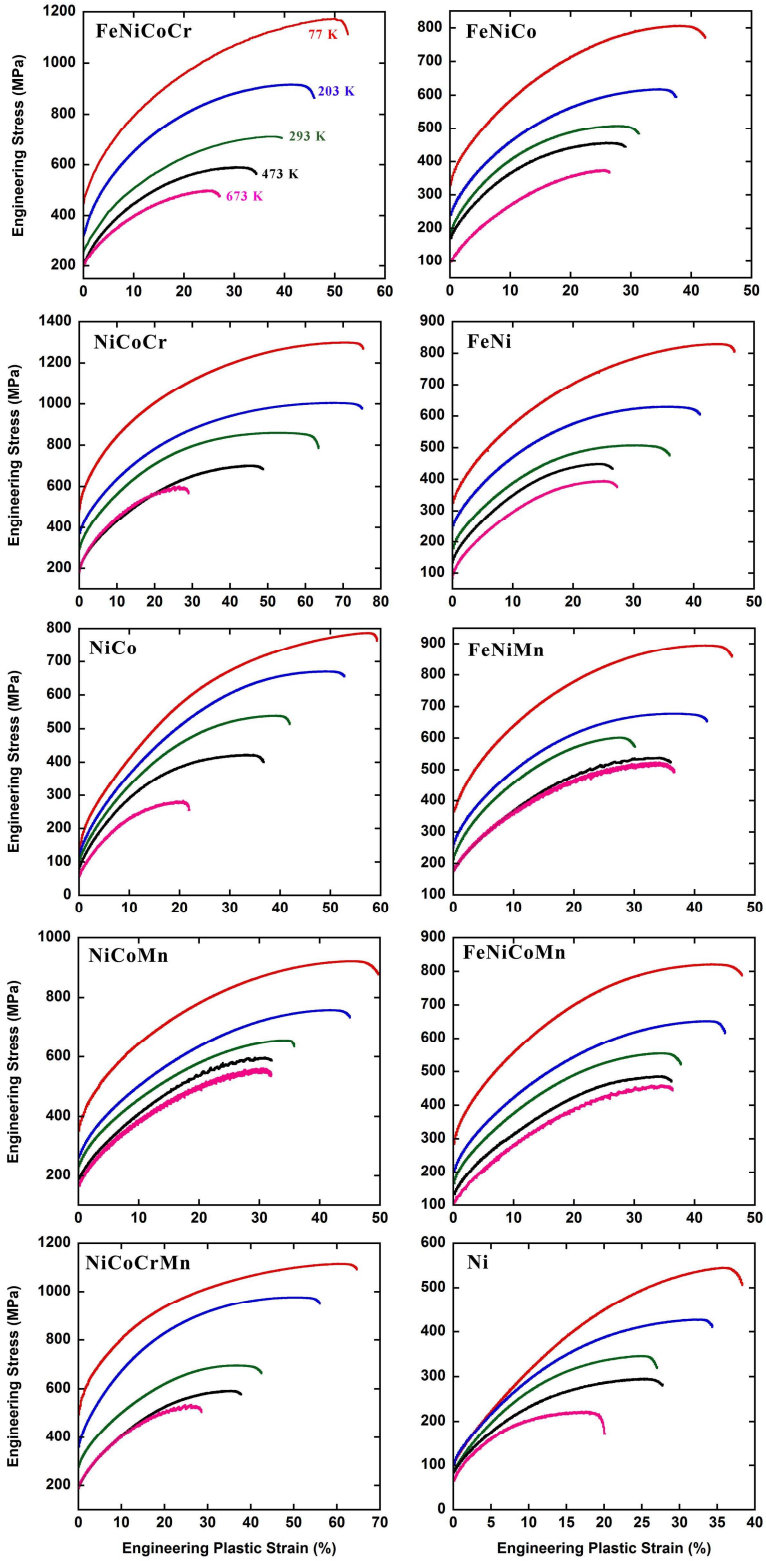

Fig. 2.2. Engineering stress vs. engineering plastic strain as a function of temperature for the equiatomic alloys.

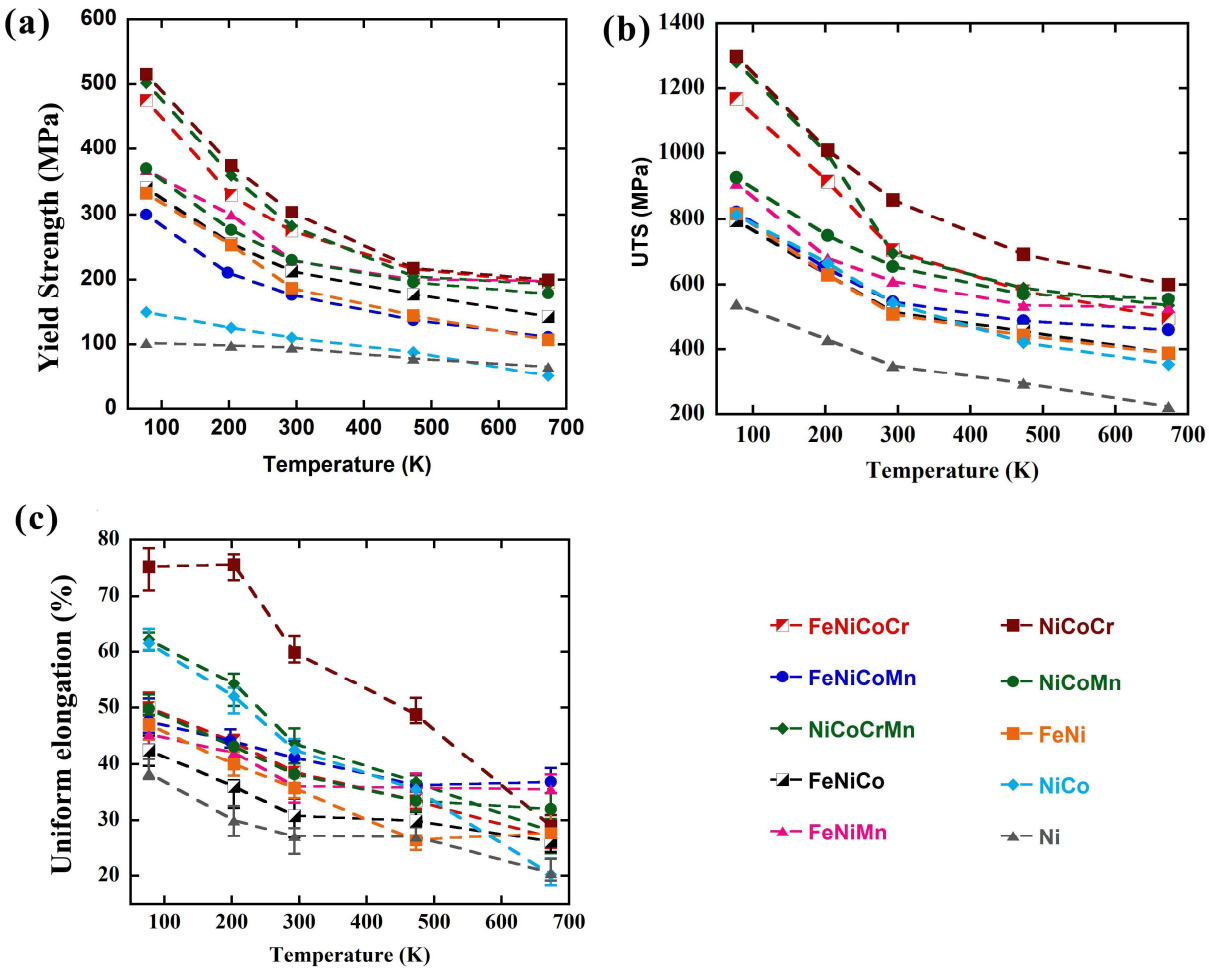

Fig. 2.3. Temperature dependence of: (a) the 0.2% offset yield stress (σ_y); (b) the ultimate tensile strength (UTS); and (c) the uniform elongation to fracture for the equiatomic alloys.

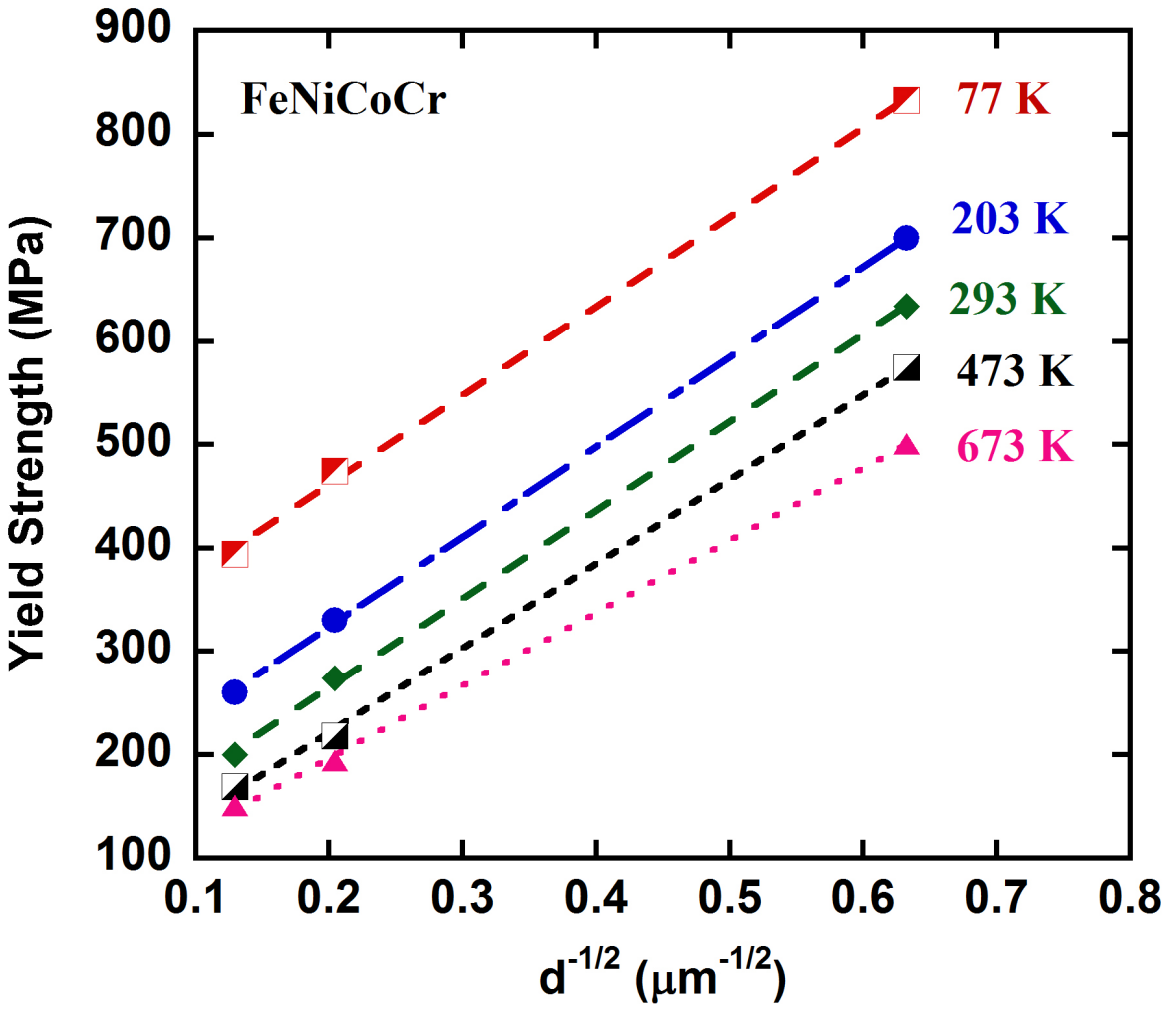

Fig. 2.4. Hall-Petch plots showing the effects of grain size, *d*, on the yield strength of the FeNiCoCr equiatomic alloy at different temperatures.

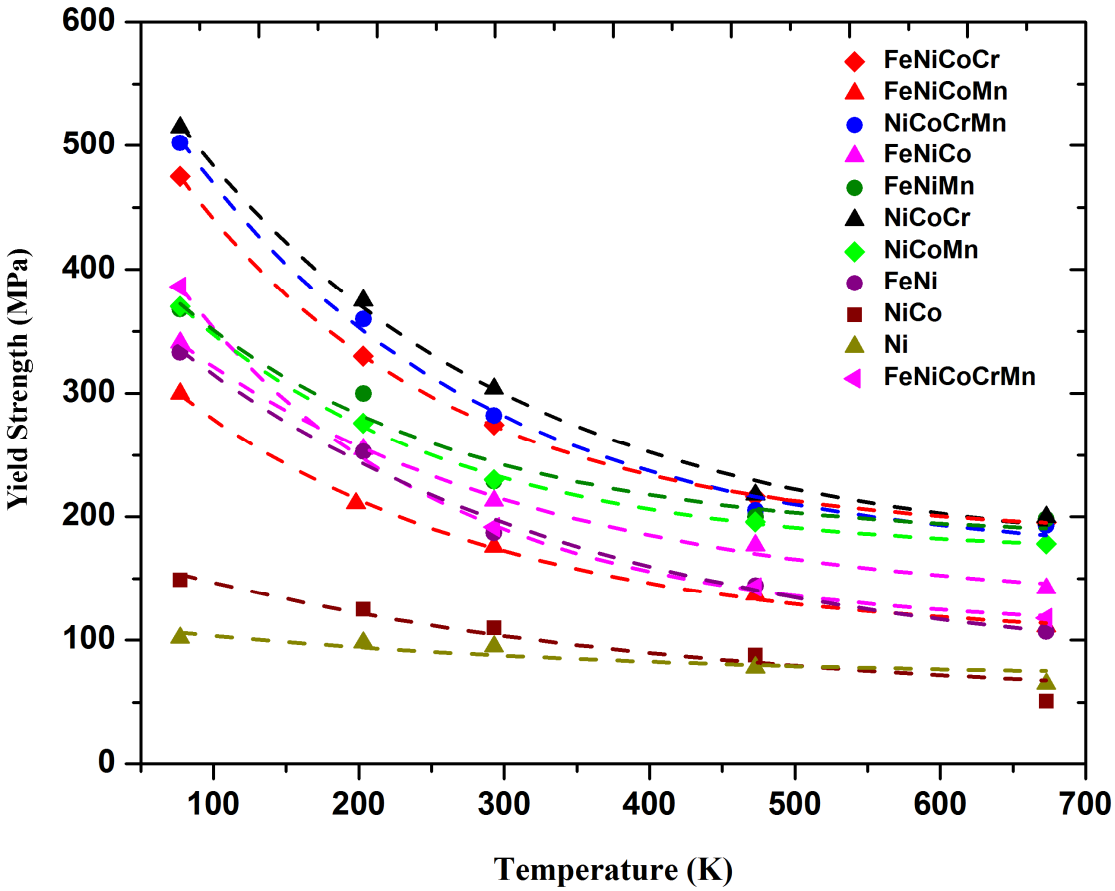

Fig. 2.5. The temperature dependence of the 0.2% offset yield stress of the equiatomic alloys and pure Ni. The dashed lines are curve fits to the form of Eq. 10. Data for the quinary alloy FeNiCoCrMn are from [26].

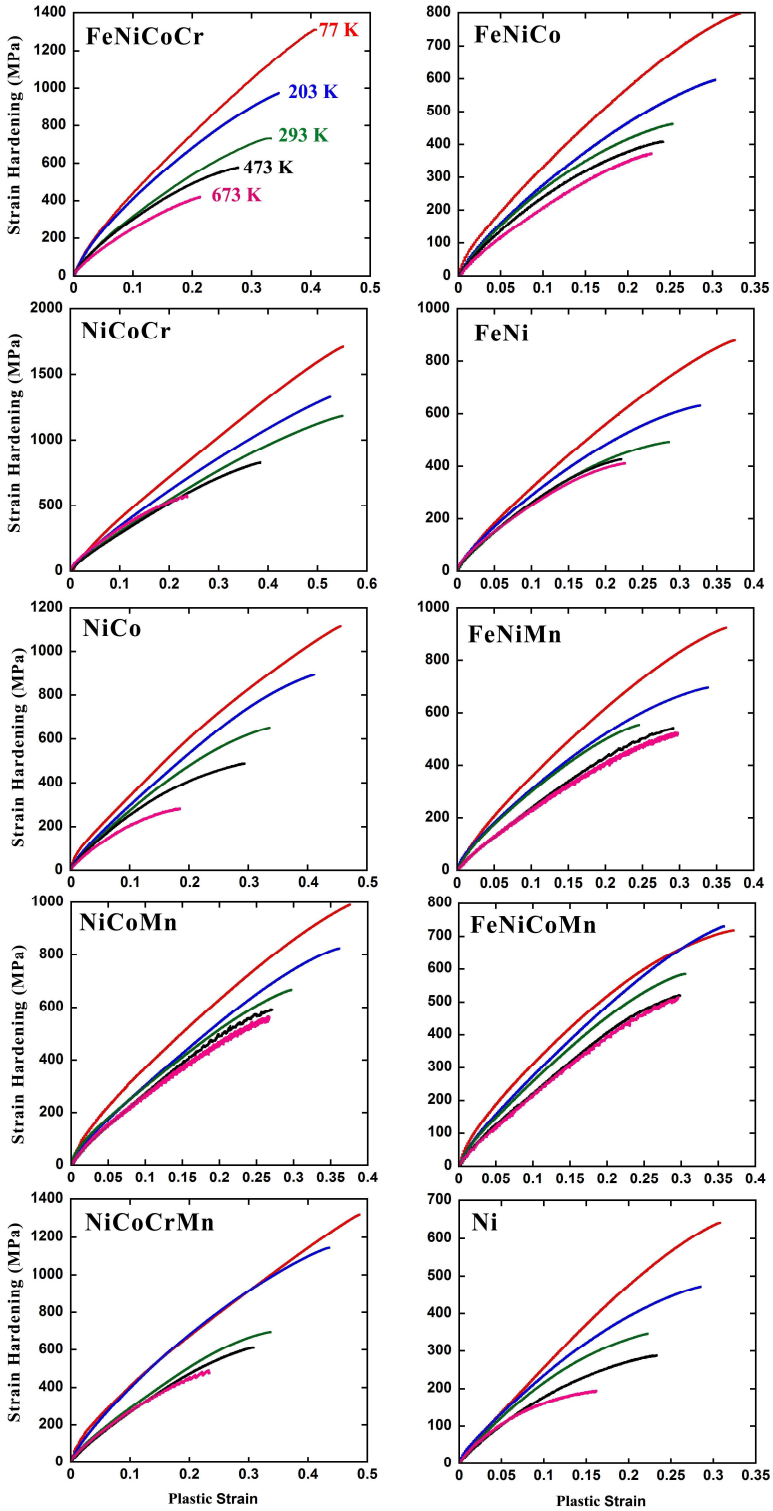

Fig. 2.6. Strain hardening portion of the flow stress ($\Delta\sigma_\rho = \sigma_{flow} - \sigma_y$) vs. true plastic strain as a function of temperature for the equiatomic alloys.

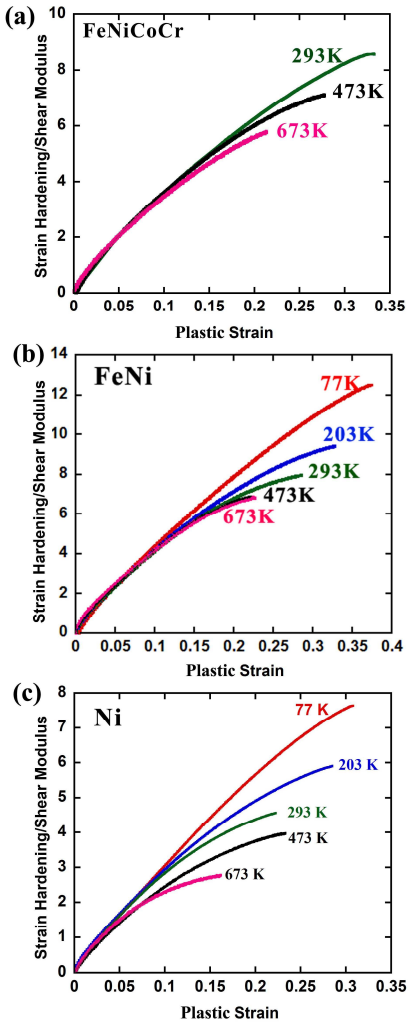

Fig. 2.7. Shear modulus corrected strain hardening versus true plastic strain curves for: (a) the FeNiCoCr equiatomic alloy; (b) the FeNi equiatomic alloy; and (c) pure Ni.

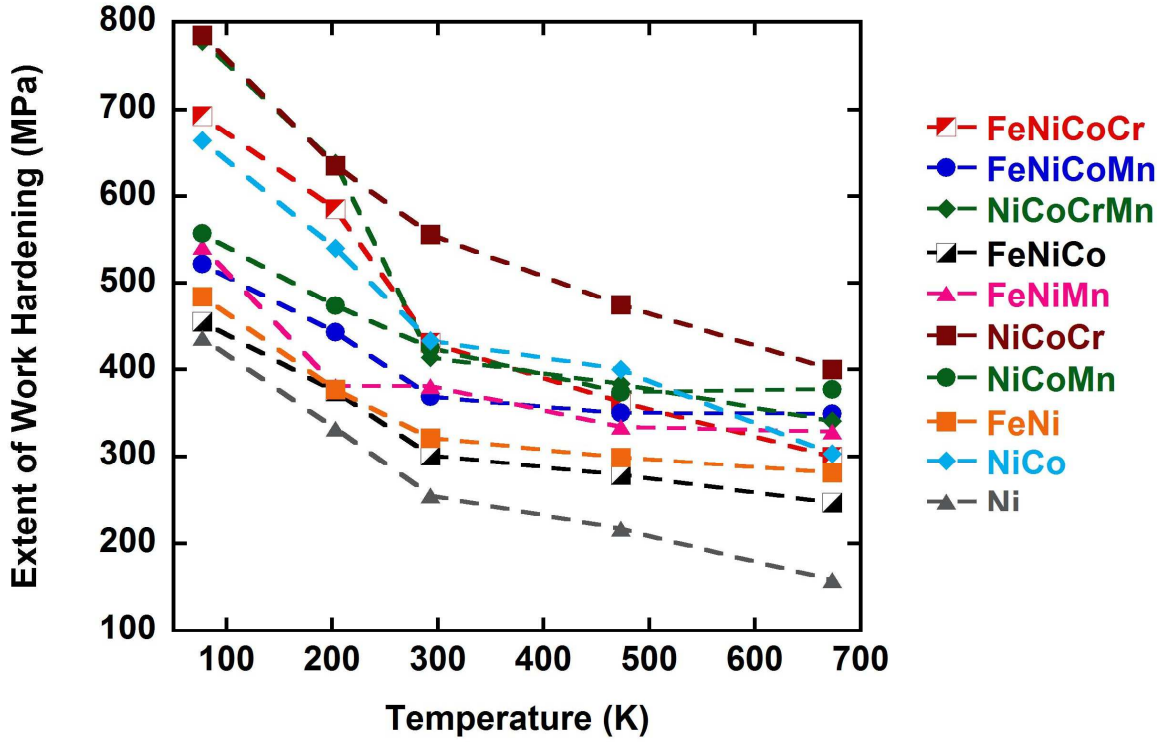

Fig. 2.8. Temperature dependence of the extent of work hardening (UTS – σ_y) for the equiatomic alloys.

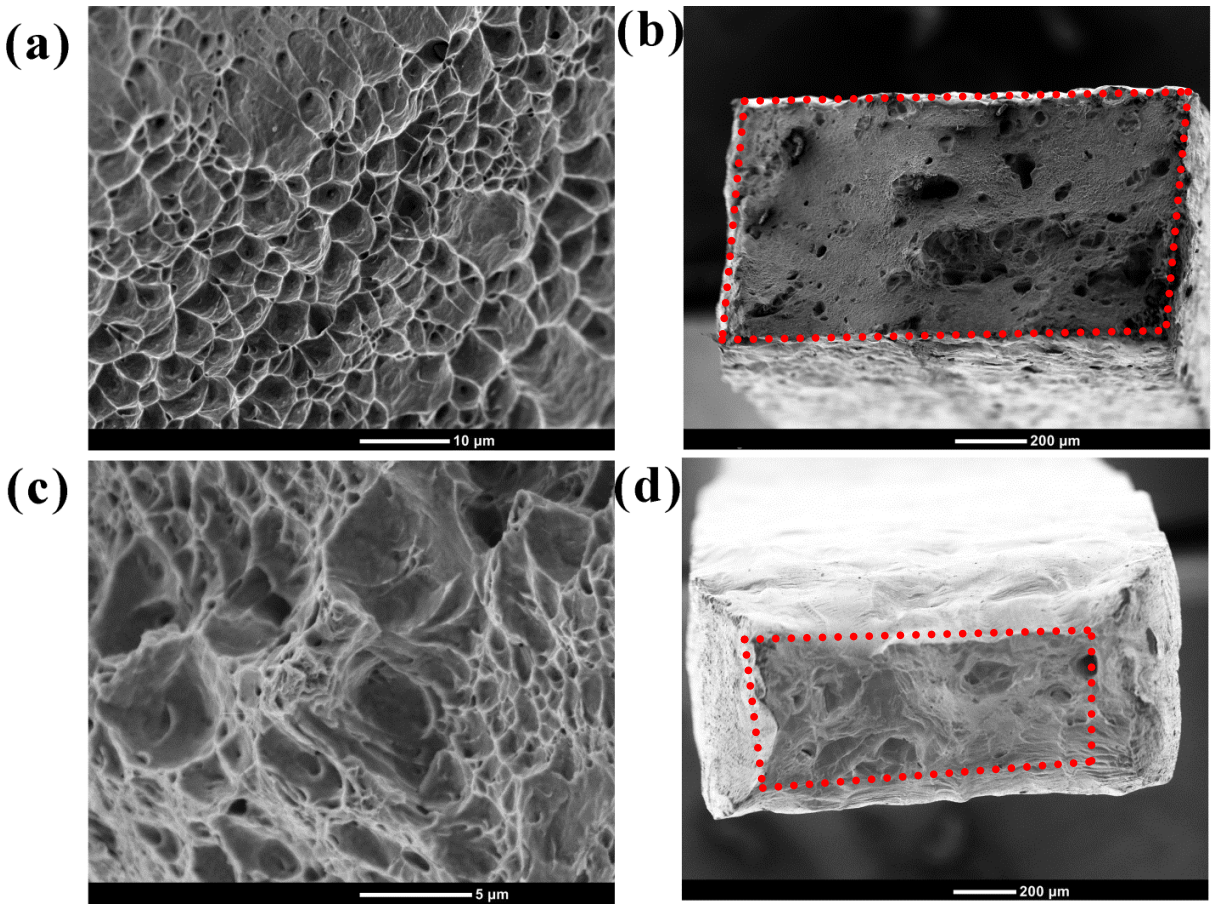

Fig. 2.9. High and low magnification fractographs of tensile samples tested to failure at 77 K: (a, b) FeNi and (c, d) Ni.

CHAPTER III

Alloying Effects on the Mechanical Properties of Equiatomic FCC Solid Solution Alloys

This article in the same form will be submitted to Scripta Materialia.

Authors:

Z. Wu

Materials Science and Engineering Department, University of Tennessee, Knoxville, TN 37996, USA

H. Bei

Materials Science and Technology Division, Oak Ridge National Laboratory, Oak Ridge, TN 37831, USA

G.M. Pharr, E.P. George

Materials Science and Engineering Department, University of Tennessee, Knoxville, TN 37996, USA; and Materials Science and Technology Division, Oak Ridge National Laboratory, Oak Ridge, TN 37831, USA

Abstract

The mechanical properties measured in uniaxial tensile tests of a family of single-phase equiatomic binary, ternary, quaternary alloys (which are subsystems of the equiatomic FeNiCoCrMn quinary alloy) have been analyzed and correlated with material parameters that can be used to help understand their behavior. The material parameters include the number of alloying elements, melting temperature, lattice parameter, Poisson's ratio, differences in atomic size and elastic modulus, and annealing twin density. Statistical procedures were used to analyze the influences of these factors and the extent to which they contribute to the differences in basic mechanical properties including yield strength, ultimate strength, work hardening, and ductility. The analysis suggests that the mechanical behavior is most highly correlated with the annealing twin density, which has effects on both the strength and strain hardening behavior, and the maximum modulus difference which correlates in a significant way with the strengths of the alloys. The strength also mildly correlates with the number of alloying elements, but it appears that the specific nature of the alloying elements is probably more important. Chromium, in particular, provides significant strengthening.

Recent experimental work has shown that it is sometimes possible to combine five or more metallic alloying elements in equal atomic proportions to obtain a single phase random solid solution alloy with a simple crystal structure such as face-centered cubic (FCC) [1]. Often referred to as high entropy alloys (HEA), it has been suggested that the reason these alloys can exist as simple single phase materials is that the entropy of mixing is large enough to overcome the enthalpy reduction associated with compound or phase formation [2]. Although the number of equiatomic alloys that exist as truly stable single-phase materials is limited, those that do often exhibit interesting mechanical properties including high strength and ductility. In addition, it has recently been shown that some FCC equiatomic alloys exhibit significant increases in strength and ductility with decreasing temperature [3-5], in contrast to pure FCC metals whose mechanical properties are usually not a strong function of temperature in the cryogenic range [6]. Another interesting characteristic of equiatomic alloys is that the mechanisms that determine their strength cannot be described by normal concepts of solid solution strengthening. This follows from the observation that when the alloying elements are present in equal atomic proportion, there is no way to distinguish between the solute and solvent species. Most theories of solid solution strengthening start from the assumption of a dilute solution of the solute in the solvent.

In a recent set of experiments, we investigated the phase stability and mechanical properties of a series of equiatomic alloys based on the FeNiCoCrMn equiatomic system [5, 7]. This quinary alloy exhibits a strong increase in strength and ductility at liquid nitrogen temperatures, possibly caused by an increased tendency for deformation twinning [4]. We have found that several subsystems of this alloy also exist as single-phase FCC random solid solutions [5], which provides an interesting opportunity to study the mechanical behavior of much simpler alloys and

explore the influence of the number of alloying elements on the properties. The specific single-phase FCC subsystems are: (1) the binary alloys FeNi and NiCo; (2) the ternary alloys FeNiCo, FeNiMn, NiCoCr, and NiCoMn; and (3) the quarternary alloys FeNiCoCr, FeNiCoMn, and NiCoCrMn. Along with the quinary FeNiCoCrMn and pure FCC Ni, this represents a set of 11 related equiatomic alloys with single phase FCC structure. We recently documented the tensile stress-strain behavior of these alloys as a function of temperature over the range 77-673K and found that the strength and ductility of all the alloys increase with decreasing temperature, but to differing degrees depending on the exact alloying combination. Curiously, the alloy with the largest solid solution strengthening effects is not the quinary but one of the ternaries, NiCoCr. This suggests that it is not necessarily the number of alloying elements that produces the strengthening effects, but rather that the nature of the specific elements is somehow important.

Here, we re-examine the mechanical property data from a statistical perspective to determine what characteristics of the alloys correlate with observed mechanical properties. The focus is on those parameters, which, from a mechanistic perspective, are known to be important in traditional descriptions of strengthening. These include the number of elements, n, the melting temperature, T_m (measured by differential scanning calorimetry), the room temperature lattice parameter, a (measured by powder x-ray diffraction), the density, ρ, (measured by pycnometry), and the shear modulus, G, and Poisson's ratio, ν, (measured by ultrasonic techniques) [5]. Since theories of solid solution strengthening are often based on differences in elastic modulus or atomic size of the alloying species, we also consider the maximum modulus difference among the alloying elements (maximum Young's modulus mismatch was used since there is no available data for the shear modulus of one of the elements, Mn), ΔE, and the maximum difference in their atomic size, Δr. For reference purposes, the polycrystalline Young's moduli, E,

for the pure elemental materials in their normal crystalline forms are E_{Fe} = 211 GPa , E_{Ni} = 200 GPa, E_{Co} = 209 GPa, E_{Cr} = 279 GPa, and E_{Mn} = 198 GPa [8], and the atomic radii are r_{Fe} = 0.1411 nm , r_{Ni} = 0.1377 nm, r_{Co} = 0.1385 nm, r_{Cr} = 0.1423 nm, and r_{Mn} = 0.1428 nm [9]. Since twinning is suspected to play a role in determining the strength of some of these materials, we also examine the annealing twin density, ρ_{twin}, as a first-order indicator of the ability of the material to twin. The annealing twin density is defined here as the number of intersections of twin boundaries by a line of unit length determined from the back-scattered scanning electron microscope images [3, 5]. Details on how these parameters were measured are provided elsewhere [5].

The mechanical properties of interest in the correlation analysis are the yield strength, σ_y, the ultimate tensile strength, σ_{uts}, the uniform percent elongation to fracture, e_f, the work hardening capability, $(\sigma_{uts}-\sigma_y)$, and the average strain hardening rate, $(\sigma_{uts}-\sigma_y)/e_f$. Because of the interest in strength and ductility at cryogenic temperatures, the parameters have been evaluated both at room temperature (RT), nominally 293 K, and liquid nitrogen (LN) temperature, 77 K.

Table 3.1 shows the basic data matrix, where the rows represent each of the equiatomic alloys and the columns are the measured material parameters. To visualize the relationships between the measured mechanical properties and the other material parameters in the matrix, scatter plots of the basic mechanical properties (rows) against the other material parameters are given in Fig. 3.1a for the room temperature properties and Fig. 3.1b for the properties at 77K. Each plot contains 11 data points, one for each of the 11 alloys. For each individual plot, the units used are those in Table 3.1. Examination of the plots shows that some parameters are highly correlated, e.g., the ultimate tensile strength and the twin density, while others are not, e.g., the yield strength and Poisson's ratio.

To statistically test the strength of the correlations, we use two commonly used correlation procedures: Pearson's product-moment correlation and Spearman's rank correlation [10, 11], both of which assume a linear relationship between the two variables. In general, the Pearson correlation is more useful than the Spearman correlation, in which the ranking rather than the actual value of the parameter is used, but for the Pearson to apply, the data must be distributed in a roughly normal fashion. To establish the extent to which the data are normally distributed, cumulative probability plots were constructed for the pair of variables and the degree of normality was visually assessed. Significant deviations from normality were observed for the maximum modulus mismatch and the maximum atomic size mismatch, so for these cases, the Spearman correlation was used. In all other cases, the Pearson correlation was applied. In order to determine the level of significance of the correlations, Student's t-test was used to measure the level of significance, *p*. It has been shown that the t-test is very robust to non-normality except for very small samples (e.g., N<5) [10]. Detailed procedures for the determination of the correlation coefficients, *r*, and the level of significance, *p*, can be found elsewhere [10, 11].

The calculated correlation coefficients (*r*) and level of significance (*p*) computed in these ways are summarized in Table 3.2. The values of *r* range between -1 and +1, representing perfect negative and positive linear relationships, respectively. When $r>0$, the two variables are positively correlated (one variable increases with an increase of the other and vice verse), and the magnitude of a correlation coefficient indicates the degree of linear correlation between the two variables. When $r<0$, the two variables are negatively correlated and one decreases as the other increases. The typical range of *r* for a very strong correlation is ±0.9 to ±1. A strong correlation exists for *r*'s in the range ±0.7 to ±0.9 and moderate correlation for ±0.5 to ±0.7 [10]. With respect to the level of significance, when $p< 0.05$, the correlation is deemed "significant" and

unlikely to have occurred by chance [10, 11]. The values *r* and *p* in Table 3.2 have been color coded to indicate the level of significance in combination with the strength of the correlation. For correlation parameters shown in black, the level of significance *p* is not less than 0.05, so the material parameters are not significantly correlated. For the fonts shown in colors, a significant correlation exists ($p<0.05$), and the correlation coefficient *r* is greater than 0.5, indicating at least a moderate degree of correlation. Correlation parameters in red are very strongly correlated ($r>0.9$ or $r<-0.9$), those in blue are strongly correlated ($0.7<r<0.9$ or $-0.9<r<-0.7$), and those in green are moderately correlated ($0.5<r<0.7$ or $-0.7<r<-0.5$).

Examination of the data in Table 3.2 shows that great majority of the mechanical properties correlate in significant ways with the annealing twin density. The highly correlated parameters include the strength, elongation, and hardening capability, all of which show statistically significant positive correlations for room temperature testing and at liquid nitrogen temperature. Assuming that the tendency to deform by twinning is linked to the tendency to form annealing twins through the stacking fault energy, many of the correlations can be explained in terms of a tendency for the material to deform by twinning mechanisms that become more pronounced at lower temperatures. In fact, it has been suggested that the formation of nano-twins during deformation at low temperatures may explain the large work hardening capability and thus the increased ultimate tensile strength of the FeNiCoCrMn alloy [4] and other alloys [12-17]. The formation of mechanical twins and their role in deformation provides additional strengthening if the twin boundaries are effective barriers to dislocation motion. Normally, deformation twinning is not observed under normal deformation conditions at room temperature in face-centered cubic (FCC) metals with medium or high stacking fault energy, γ_{SFE}, such as Al [18]. However, at low temperatures (LN), materials with moderate stacking fault energies do form mechanical twins.

One such example is Cu [19], whose stacking fault energy is ~ 80mJ/m^2 [20]. Fe, Co, Cr and Mn have all been shown to reduce the stacking fault energy of nickel, with Cr having the largest effect and Fe the smallest [21, 22]. Based on this, one could argue that the equiatomic FeNi alloy should have a relatively high stacking fault energy and NiCoCr a low one, consistent with the observation that the annealing twin density in FeNi is relatively low while that in NiCoCr is high. Thus, the differences in strength at low temperatures among the equiatomic alloys examined here could be reasonably attributed to differences of stacking fault energy caused by alloying that affects the work hardening behavior through the promotion of twinning activity. The onset of deformation twinning would also postpone necking instability and hence increase the ductility, resulting in a strong correlation between the ductility and annealing twin density, as observed in some of the alloys.

The parameters in Table 3.2 also suggest that there is a moderate to strong correlation between the many of the mechanical properties, especially the yield strength and ultimate tensile strength, both at room temperature and at liquid nitrogen temperature, and the maximum modulus mismatch in the alloying elements. Curiously, there are essentially no significant correlations between mechanical properties and the maximum atomic size mismatch, as is often the case in solid solution strengthening. However, this is not particularly surprising given that all 5 of the elements are essentially the same size, varying by only 3.7% at most. The maximum modulus mismatch in the alloys is as high as ~40%, with the larger mismatches occurring in the Cr containing alloys (Cr has by far the largest modulus of the five elements). These observations are consistent with conventional theories of solid solution strengthening that attribute the strengthening effects largely to modulus and atomic size mismatch. On the other hand, it is clear from the scatter plots in Fig. 3.1 and the data collection matrix in Table 3.1 that the maximum

modulus mismatch alone cannot explain the differences in strength. For instance, the equiatomic FeNiCoCrMn, FeNiCoCr, NiCoCrMn and NiCoCr alloys all have the same or similar maximum modulus mismatch of 40.9%, 39.5%, 40.9% and 39.5%, respectively, but their yield strengths vary over a large range from 215 MPa for FeNiCoCrMn to 304 MPa for NiCoCr.

Lastly, given that it has been suggested that the number of elements in a single phase equiatomic alloy may correlate with its strength due to the potential for more complex lattice distortions when the number of alloying elements is high [2], a comment is warranted on the relationship between the number of elements in the alloys and their mechanical properties. Table 3.2 indicates that there indeed is a statistically significant, positive correlation between number of elements and the yield strength of the alloys, and to a lesser extent the ultimate tensile strength. However, there are notable exceptions to this correlation. Specifically, the material with the greatest yield strength at all temperatures is the ternary NiCoCr, whereas the yield strength of the quinary FeNiCoCrMn alloy is essentially in the middle of the alloys [3]. In addition, for the ternary alloys, the yield strength of the NiCoCr alloy (304 MPa) is much higher than that of FeNiCo (213 MPa), and this phenomenon is also observed for the FeNiCoMn (176 MPa) and NiCoCrMn (282MPa) quarternary alloys. In both cases, the only compositional difference is that the replacement of Fe with Cr, indicating a much more pronounced strengthening effect of Cr than Fe in the alloys. A large strengthening effect of Cr relative to Mn is also observed by comparing the two ternary alloys, NiCoMn (230 MPa) and NiCoCr (304 MPa), and two quaternary alloys, FeNiCoMn (176 MPa) and FeNiCoCr (274 MPa). Thus, when it comes to strength, it is clear that the nature of the alloying elements is just as important or more important that the number of elements, with Cr appearing to be a significant strengthener in this system of

alloys, possibly due to its much larger elastic modulus. The circled data points in Fig. 3.1 identify the Cr containing alloys, and show that they are almost all associated with high strength.

In summary, a statistical analysis was used to investigate alloying effects on the mechanical properties of a family of FCC-structured equiatomic alloys. Numerous physical and microstructural parameters were analyzed to establish statistically significant correlations with basic mechanical properties at 293K and 77K. Scatter plots were made for each pair of parameters to visualize the potential correlations followed by calculations of the correlation coefficient and level of significance determined using standard statistical procedures. Some mechanical properties were found to correlate in significant ways with two primary material parameters, the annealing twin density and the maximum modulus mismatch, and mildly with the number of alloying elements. It appears, however, that the nature of the alloying elements is just as important as the number of alloying elements, with Cr containing alloys generally being stronger, possibly due to its much larger modulus. Further investigations are needed understand the fundamental nature of strengthening in equiatomic alloys since simple solid solution strengthening concepts appear to be inadequate.

Acknowledgments: This research was supported by the U.S. Department of Energy, Office of Basic Energy Sciences, Materials Sciences and Engineering Division.

References

[1] Cantor B, Chang ITH, Knight P, et al. Mater Sci Eng A 2004; 375-377: 213.

[2] Yeh JW, Chen SK, Lin SJ, et al. Adv Eng Mater 2004; 6: 299.

[3] Gali A, George EP. Intermetallics 2013; 39:74.

[4] Otto F, Dlouhy A, Somsen Ch, et al. Acta Mater2013; 61: 5743.

[5] Wu Z, Bei H, Pharr GM, et al. Submitted to Acta Mater 2014.

[6] Low JR. Behavior of Metals at LowTemperatures.ASM. 1952, p48.

[7] Wu Z, Bei H, Otto F, et al. Intermetallics 2014; 46:131.

[8] King HW. J Mater Sci 1966; 1: 79.

[9] http://www.webelements.com/

[10] Chiang CL. Statistical Methods of Analysis. World Scientific 2003.

[11] Lomax RG. An Introduction to Statistical Concepts for Education and Behavioral Science.Lawrence Erlbaum Associates 2001.

[12] Rémy L, Pineau A. Mater SciEng 1976;26:123.

[13] Rémy L. ActaMetall 1978;26:443.

[14] Asgari S, El-Danaf E, Kalidindi R, Doherty R. Metall Mater Trans A 1997;28:1781.

[15] Rohatgi A, Vecchio KS, Gray GT. Metall Mater Trans A 2001;32:135.

[16] Beladi H, Timokhina IB, Estrin Y, Kim J, De Cooman BC, Kim SK. Acta Mater 2011;59:7787.

[17] Gutierrez-Urrutia I, Raabe D. Acta Mater 2011;59:6449.

[18] Huang CX, Wang K, Wu SD, et. al. Acta Mater 2006; 54: 655.

[19] Weiner D. Acta Metall 1972; 20: 1235

[20] Dieter GE. Mechanical Metallurgy.McGraw-Hill Higher Education. 1986

[21] Kotval PS, Nostor OH. TMS-AIME 1969; 245: 1275.

[22] Gallagher PCJ. Metall Trans 1970; 1: 2429.

Appendix 3.1

Table 3.1.Data matrix, which includes the number of elements (*n*), melting temperature (T_m), lattice parameter (*a*), Poisson's ratio (ν), shear modulus (*G*), maximum size and modulus mismatch (Δr and ΔE), annealing twin density (ρ_{twin}), yield strength (σ_y), ultimate tensile strength (σ_{uts}), elongation (e_f) and average rate of work hardening ($(\sigma_{uts}- \sigma_y)/e_f$).

	n	T_m [5] (K)	a (Å)	ρ (g/cm^3)	ν [5]	G (GPa) [5]	Δr (%)	ΔE (%)	ρ_{twin} (mm^{-1})	σ_y(RT) (MPa)	σ_{uts}(RT) (MPa)	e_f	$\sigma_{uts} - \sigma_y$ (RT) (MPa)	$(\sigma_{uts} - \sigma_y)/ e_f$ (RT)	σ_y(LN) (MPa)	σ_{uts}(LN) (MPa)	e_f (LN)	$\sigma_{uts}- \sigma_y$ (LN) (MPa)	$(\sigma_{uts} - \sigma_y)/ e_f$ (MPa) (LN)
FeNiCoCrMn [3]	5	1553	3.5991	7.9792	0.26	80	3.7	40.9	19	215	595	0.39	380	974	432	1050	0.62	618	996
FeNiCoCr	4	1695	3.5715	8.1435	0.28	82	3.34	39.5	31.2	274	705	0.38	431	1119	474	1167	0.50	693	1386
FeNiCoMn	4	1533	3.5919	8.1603	0.22	77	3.7	6.6	13	176	545	0.41	369	895	300	822	0.48	522	1096
NiCoCrMn	4	1489	3.5892	7.9635	0.25	78	3.7	40.9	35.3	282	696	0.44	414	947	502	1280	0.62	778	1250
FeNiCo	3	1724	3.569	8.3904	0.35	60	2.47	5.5	6	213	514	0.31	301	977	341	796	0.43	455	1069
NiCoCr	3	1690	3.559	8.2726	0.3	87	3.34	39.5	38. 2	304	860	0.59	556	928	515	1300	0.75	785	1043
FeNiMn	3	1473	3.616	7.8429	0.24	73	3.7	6.6	12	229	610	0.36	381	1058	368	910	0.45	542	1193
NiCoMn	3	1462	3.5977	8.1694	0.23	77	3.7	5.5	21	230	655	0.38	425	1112	370	927	0.50	557	1118
FeNi	2	1703	3.5826	8.2326	0.34	61	2.47	5.5	7	187	508	0.36	321	899	333	817	0.47	484	1027
NiCo	2	1735	3.5345	8.8484	0.29	84	0.58	4.5	24	110	543	0.43	433	1016	149	813	0.62	664	1079
Ni	1	1728	3.5238	8.908	0.31	76	0	0	5	95	350	0.27	255	940	102	538	0.38	436	1134

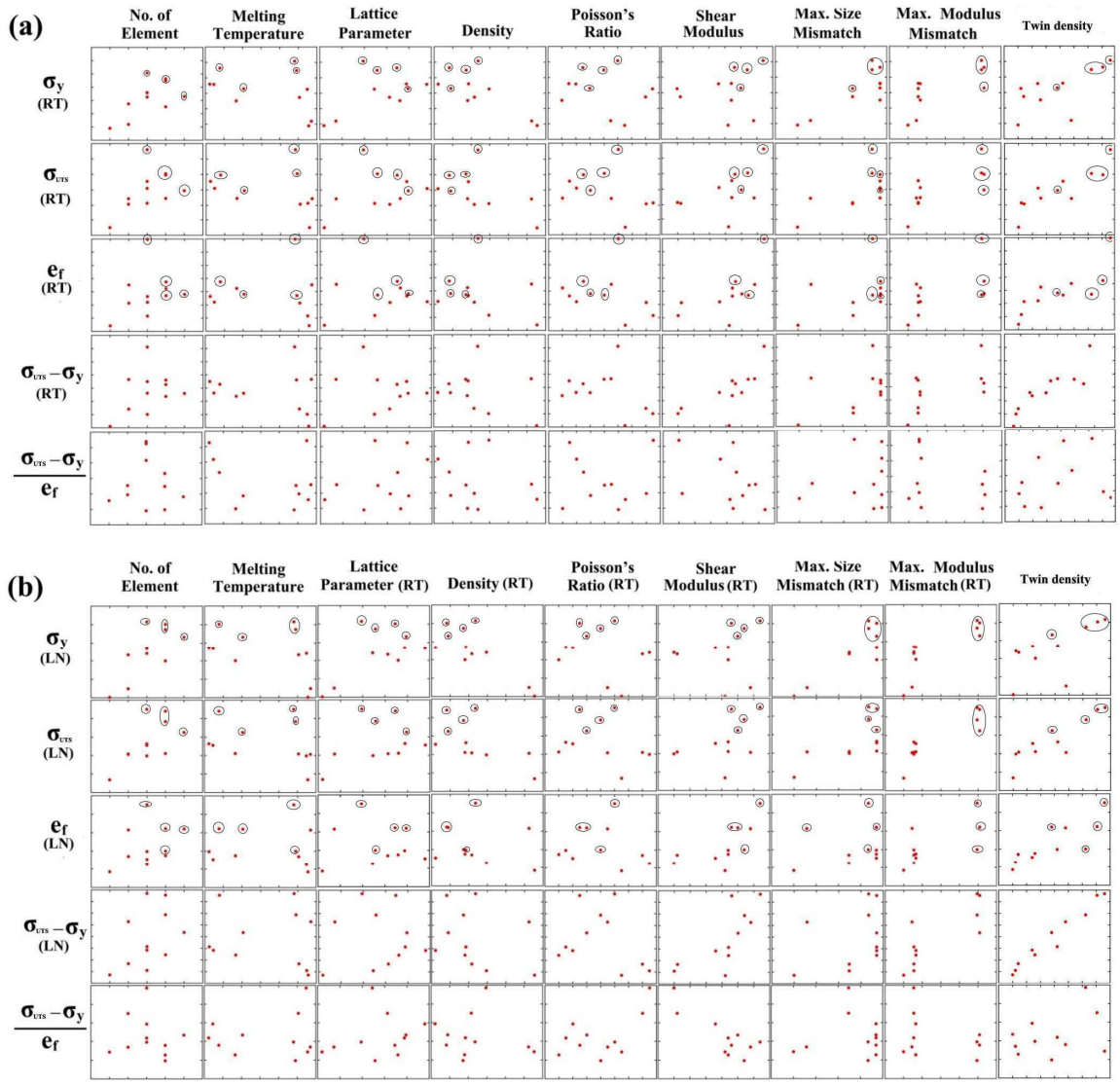

Fig. 3.1. Scatterplots in which the horizontal axis is the basic measured material parameter and the vertical axis is the mechanical property of interest. The blue circles identify alloys containing Cr.

Table 3.2. Correlation coefficients, *r*, and level of significance, *p*, for each of the correlations.

		No.of elements	Melting point	Lattice parameter	Density	Poisson's ratio	Shear modulus	Max size mismatch	Max modulus mismatch	Twin density
Yield stress(RT)	r	0.62	-0.58	0.53	-0.75	-0.20	0.18	0.54	0.74	0.6646
	p	0.0429	0.0604	0.0949	0.085	0.5582	0.6006	0.0854	0.0093	0.0257
Yield stress (LN)	r	0.73	-0.52	0.59	-0.80	-0.22	0.17	0.54	0.84	0.6422
	p	0.0113	0.1025	0.0553	0.28	0.5178	0.6245	0.0854	0.0013	0.0331
UTS(RT)	r	0.52	-0.58	0.33	-0.54	-0.30	0.52	0.58	0.73	0.8688
	p	0.0991	0.0604	0.3170	0.0856	0.3765	0.0990	0.0589	0.0108	0.0005
UTS (LN)	r	0.65	-0.59	0.35	-0.61	-0.27	0.48	0.63	0.86	0.8897
	p	0.0298	0.0556	0.2864	0.0472	0.4258	0.1341	0.0368	0.0006	0.0002
Elongation(RT)	r	0.31	-0.25	0.05	-0.23	-0.21	0.64	0.38	0.59	0.8115
	p	0.0991	0.0604	0.3170	0.0856	0.3765	0.0990	0.0589	0.0108	0.0024
Elongation (LN)	r	0.37	-0.24	-0.02	-0.17	-0.14	0.66	0.36	0.68	0.8283
	p	0.2678	0.4841	0.9604	0.6200	0.6816	0.0266	0.2709	0.0216	0.0016
hardening capability(RT)	r	0.35	-0.21	0.11	-0.28	-0.33	0.72	0.22	0.35	0.8867
	p	0.2863	0.5372	0.7382	0.4062	0.3290	0.0131	0.5243	0.2898	0.0002
Hardening capability (LN)	r	0.44	-0.27	0.02	-0.27	-0.27	0.73	0.35	0.67	0.9799
	p	0.1752	0.4171	0.9428	0.4151	0.4267	0.0115	0.2917	0.0255	0.0000001
Average strain hardening rate (RT)	r	0.3544	-0.2727	0.3405	-0.3530	-0.3083	0.2252	0.1102	0.0046	0.2248
	p	0.2848	0.4171	0.3055	0.2868	0.3562	0.5055	0.7470	0.9892	0.5063
Average strain hardening rate (LN)	r	0.2406	-0.2	-0.0029	-0.2069	-0.1766	0.3858	01629	0.0554	0.3646
	p	0.4760	0.5554	0.9930	0.5415	0.6032	0.2411	0.6322	0.8713	0.2702

SUMMARY and CONCLUSIONS

Decades-old theories of solid solution strengthening have focused on binary dilute solid solutions. In sharp contrast, the mechanical behavior of concentrated solid solutions is relatively poorly understood. During the past decade, special subsets of concentrated solute solutions in which the constituent elements are present in equal atomic proportions have received a great deal of attention. A unique feature of equiatomic alloys is the absence of “solvent” and “solute” atoms which results in a breakdown of the textbook picture of dislocations moving through a solvent lattice and encountering discrete solute obstacles. One example is the equiatomic quinary alloy, FeNiCoCrMn, in which a strong temperature dependence of strength was observed, unlike in pure FCC metals where no such dependence is typical seen. Interestingly, the ductility increased hand in hand with strength as the temperature decreased from room temperature to liquid nitrogen temperature. Through microstructural characterization, strain-induced nano-twinning at liquid nitrogen temperature was observed to be responsible for the observed large strain hardening and thus the high UTS and elongation. However, a mechanistic understanding of the temperature sensitivity of yield strength is still not clear. Thus, to have a better understanding of the aforementioned temperature dependent behavior and to develop better theories of solid solution strengthening, we investigated the temperature dependence of the mechanical properties of a family of multi-component equiatomic alloys, which are subsets of the constituent elements in the “parent” FeNiCoCrMn alloy.

After excluding a few alloys that are not able to solidify as a pure FCC solid solution based on available phase diagrams, all other binary, ternary, and quaternary alloys were drop-cast and homogenized, followed by phase identification using powder x-ray diffraction and back-scattered SEM. It was shown that, after drop-casting and homogenization, three quaternaries,

FeNiCoCr, FeNiCoMn, and NiCoCrMn, five ternaries, FeNiCo, FeNiCr, FeNiMn, NiCoCr, and NiCoMn, and two binaries, FeNi and NiCo, are single-phase FCC solid solutions. The FCC subsets of FeNiCoCr were selected to investigate their phase stabilities and recovery, recrystallization and grain growth behaviors. These alloys were cold-rolled and annealed at 300-1100 ^{o}C for 1 hour to investigate their phase stabilities. Phase separation occurs in one alloy, FeNiCr, when it is cold rolled and annealed (recrystallized), while all the others, FeNiCoCr, FeNiCo, NiCoCr, FeNi and NiCo, remain as single-phase FCC solid solutions. FeNiCo and Ni exhibit abnormal grain growth at relatively low annealing temperatures while all the other alloys show normal grain growth behavior. Under 900 ^{o}C, the grain growth exponents of the equiatomic alloys FeNiCoCr, FeNiCo, NiCoCr, FeNi, and NiCo are ~0.25, compared to ~0.5 for pure Ni, suggesting that solute drag may alter the grain growth kinetics of the equiatomic alloys. All the investigated equiatomic alloys, FeNiCoCr, FeNiCo, NiCoCr, FeNi and NiCo, as well as pure Ni show a Hall-Petch type of grain size dependence of microhardness. The ternary equiatomic alloy NiCoCr is harder than all the other alloys, including the quaternary alloy FeNiCoCr, suggesting that solid solution hardening in multi-component equiatomic alloys cannot be solely determined by the number of alloying elements, rather the type of alloying element is also important.

For those alloys identified as FCC single phase solid solutions, the mechanical properties were investigated as a function of temperature. The alloys were arc-melted, drop-cast, homogenized, cold-rolled, and recrystallized to produce equiaxed microstructures with comparable grain sizes. Tensile tests were performed at an engineering strain rate of 10^{-3} s^{-1} at temperatures in the range 77-673 K. Their melting temperatures, shear moduli and Poisson's ratios were measured to help us understand and analyze the data. Generally speaking, there are two effects on the mechanical properties: temperature effects and alloying effects. The flow stress of the equiatomic alloys is

temperature dependent to varying degrees and arises from the temperature-dependence of both yield strength and strain hardening. The temperature dependence of the yield strength in the alloys may be determined by Peierls-barrier-dominated lattice friction, with the height of the Peierls barrier controlled by thermal influences on the width of the dislocation. By fitting the experimental yield stress vs. temperature curves to the Peierls-Nabarro equation, the Peierls barriers in the equiatomic FCC alloys appear to be stronger than those in pure FCC metals but weaker than those in pure BCC metals. During the initial stages of plastic deformation (5-13% strain, depending on material), the temperature dependence of strain hardening is due almost entirely to the temperature dependence of the shear modulus. This indicates the athermal nature of dislocation multiplication, accumulation and interaction during the early stages of deformation. The ultimate tensile strength and uniform elongation to fracture of all the equiatomic alloys increase with decreasing temperature, with the largest increase occurring between 77 and 293 K. It is possible that deformation twinning similar to that observed in the FeNiCoCrMn high-entropy alloy contributes to the enhanced ductility at cryogenic temperatures in some of the alloys.

Alloying affects both the thermal and athermal portions of the yield stress vs. temperature curves. With similar grain size, the stronger alloys are not necessarily the ones with the most elements. The nature of the constituent elements also matters\, with the Cr-containing alloys in general being the strongest. To have a better understanding of the compositional effects, the physical properties (density, melting temperature), elastic properties (shear modulus, Poisson's ratio), crystal structure parameter (lattice constant) and microstructural parameter (annealing twin density) were collected in a matrix, in which the maximum modulus and size mismatch were also included, together with the mechanical properties deformed at room temperature and

low temperature. A statistical method was used to determine that what characteristics of the alloys may specifically correlate with the observed mechanical properties. Scatterplots were made for each pair of parameters to visualize their correlation followed by calculations of correlation coefficient and level of significance to measure the strength and significance of their correlations. Some mechanical properties were found to correlate in significant ways with two primary material parameters, the annealing twin density and the maximum modulus mismatch, and mildly with the number of alloying elements. It appears, however, that the nature of the alloying elements is more important than the number of alloying elements, with Cr containing alloys generally being stronger. Further investigations are needed to understand the fundamental nature of strengthening in these alloys since simple solid solution strengthening concepts are not adequate.

VITA

Zhenggang Wu was born in China in 1987. He was raised in Wuxue, Hubei, China. After graduating from Wuxue High School, Wuxue, Hubei, China in 2004, Zhenggang enrolled in the Powder Metallurgy Research Institute at Central South University, Changsha, Hunan, China, where he earned his Bachelor's Degree in Materials Science in 2008. In 2009, he started to pursue a doctorate in Materials Science and Engineering at the University of Tennessee. He received a Ph.D. degree under the guidance of Dr. George M. Pharr in 2014.